# 15TH ASSEMBLY OF PETROLOGY AND GEOCHEMISTRY

Nagybörzsöny – Banská Štiavnica

2-4 October 2025

*"The whispers of rock, stories from the Earth"*

Nagybörzsöny
Banská Štiavnica
2025
15th ASSEMBLY of PETROLOGY and GEOCHEMISTRY

# EXCURSION GUIDE

**15th Assembly of Petrology and Geochemistry, Excursion Guide**

**Editors**

Attila VIRÁG, Barbara CSERÉP, Kata MOLNÁR, Máté SZEMERÉDI

**Conference Organizers**

Réka LUKÁCS[1,2] (Head of the Organizing Committee)

Barbara CSERÉP[1,2], György CZUPPON[1], Péter GÁL[1,2], Krisztina HAJDU[1,2], Szabolcs HARANGI[1,2], Máté KARLIK[3], Ivett KOVÁCS[1], Emese OELBERG-PÁNCZÉL[1,2], János SZEPESI[1,4], Máté SZEMERÉDI[1,5], Kata TEMOVSKI-MOLNÁR[1,4], Attila VIRÁG[1,2]

Igor BROSKA[6], Milan KOHÚT[6], Samuel RYBÁR[7,8], Katarína ŠARINOVÁ[9]

[1] MTA–HUN-REN CSFK Lendület "Momentum" PannonianVolcano Research Group
[2] Department of Petrology & Geochemistry, Institute of Geography and Earth Sciences, Eötvös Loránd University
[3] HUN-REN Research Centre for Astronomy and Earth Sciences, Institute for Geological and Geochemical Research
[4] HUN-REN Geochronology Group, Institute for Nuclear Research (ATOMKI)
[5] Department of Geology, 'Vulcano' Petrology and Geochemistry Research Group, University of Szeged
[6] Earth Science Institute of the Slovak Academy of Sciences
[7] Department of Geology and Paleontology, Faculty of Natural Sciences, Comenius University
[8] Department of Geodesy and Mine Surveying, Faculty of Mining and Geology, Technical University of Ostrava
[9] Department of Mineralogy, Petrology and Economic Geology, Faculty of Natural Sciences, Comenius University

The **Assembly of Petrology and Geochemistry** is an official event of the *Subcommittee on Petrology* of the *Committee on Geochemistry, Mineralogy and Petrology* of the *Hungarian Academy of Sciences* and the *Mineralogy, Petrology and Geochemistry Section* of the *Hungarian Geological Society*.

**Motto**

*Anjana Khatwa*

**Cover Art**

*The Calvary of Banská Štiavnica (Photo: Jaroslav LEXA)*

# EXCURSION GUIDE

# GEOLOGY AND VOLCANIC ROCKS OF THE ŠTIAVNICA COMPOSITE VOLCANO

Jaroslav Lexa
Earth Science Institute, Slovak Academy of Sciences, Bratislava, Slovakia

## 1. Itinerary

**Leader: Jaroslav LEXA**

8:00: Departure from Nagybörzsöny

9:00 - 12:30: Morning excursion

Medovarce – the 1st pre-caldera stage, Sebechleby Formation: succession of shallow marine epiclastic volcanic conglomerates/sandstones and inter-bedded lahar deposits.

Ladzany – the 4th post-caldera stage, Baďan Formation: pyroxene andesite lava flow

Brhlovce – the 4th post-caldera stage, Baďan Formation: succession of shallow marine reworked pumice tuffs, pumiceous sandstones and epiclastic volcanic sandstones

Počúvadlo – the 4th post-caldera stage, Biely kameň Formation: welded ignimbrite of biotite-amphibole-orthopyroxene andesite.

12:30 - 13:00: Lunch (lunch-packs)

13:00 - 18:00: Afternoon excursion

Šementlov – the 2nd stage of subvolcanic intrusions, Zlatno Intrusive Complex: granodiorite porphyry stock/dike showing a porphyry system quartz-sericite-pyrite alteration.

Hodruša – Mayer shaft – the 2nd stage of subvolcanic intrusions, Hodruša-Štiavnica intrusive complex: top of the granodiorite bell-jar pluton

Hodruša – tajch – the 2nd stage of subvolcanic intrusions, Banisko Intrusive Complex: bt-amph quartz-diorite porphyry sill.

Juraj adit – the 2nd stage of subvolcanic intrusions, Banisko Intrusive Complex: bt-amph quartz-diorite porphyry ring dike

Banský Studenec – the 3rd caldera stage, Studenec Formation: bt-amp andesite extrusive dome

Ilija – the 3rd caldera stage, Studenec Formation: bt-amph andesite pumice flow deposits

18:00: Guided tour in Banská Štiavnica and Gala Dinner

## 2. Structure and evolution of the Štiavnica Stratovolcano

The Štiavnica Stratovolcano is the most extensive and complex volcanic edifice among the Miocene to Quaternary volcanoes of the Carpathian-Pannonian region that hosts the world-class Banská Štiavnica - Hodruša ore district. It has well-preserved volcanic formations and complexes in the proximal and distal zones (Fig. 1) that allowed for a serious paleovolcanic reconstruction (Konečný et al., 1998; Chernyshev et al., 2013). A resurgent horst in the central part of its caldera exposes subvolcanic intrusive complexes and related ore mineralizations (Fig. 2).

The edifice of the Štiavnica Stratovolcano represents a succession of volcanic formations and complexes with a common central zone and outward dipping volcanic slopes that corresponds to the protracted evolution of a transcrustal magmatic system (Rottier et al., 2020). Its structure and evolution in five essential stages, originally compiled by Konečný et al. (1998a,b) has been recently treated by Chernyshev et al. (2013) and Lexa et al. (2025). Note, that a legend of the Fig. 1 includes a subdivision of the stratovolcano into lithostratigrapic units and their brief lithologic/petrographic description. Evolutiuon of the stratovolcano is summarized in the Fig. 3.

During the **1st or pre-caldera stage** (dated to 15.0–13.6 Ma) volcanic activity of px and amph-px andesites, interrupted by periods of quiescence and related erosion, created a succession of stratovolcanic complexes and formations. Paleovolcanic reconstruction points to remnants of a large stratovolcanic edifice, 40 km in diameter at the base of a compound volcanic cone, surrounded by accumulations of epiclastic volcanic rocks.

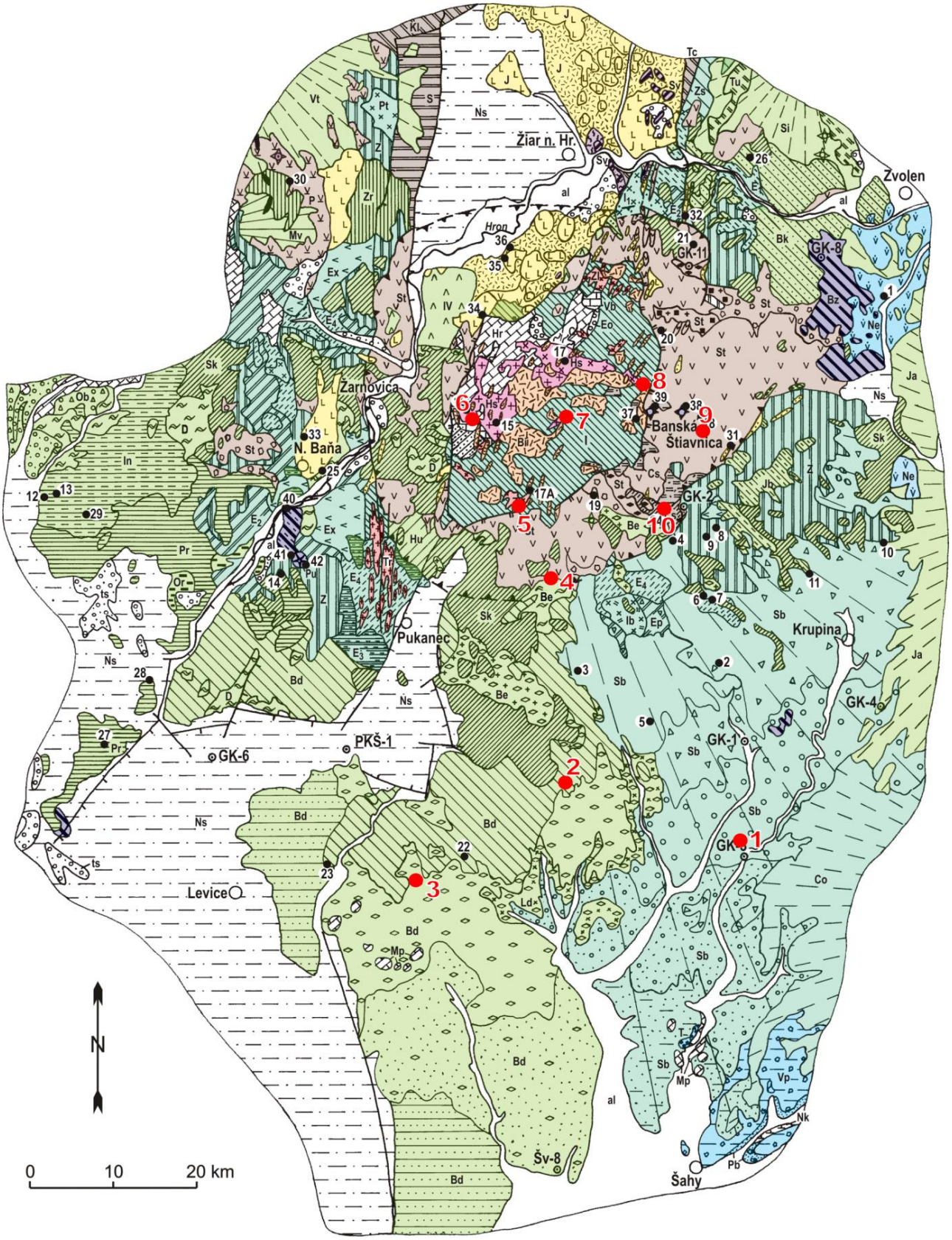


***Figure 1a.*** *Structural scheme of the Štiavnica Stratovolcano (Chernyshev et al. 2013). Red dots indicate visited localities. See the legend on the next page (Fig. 1b).*

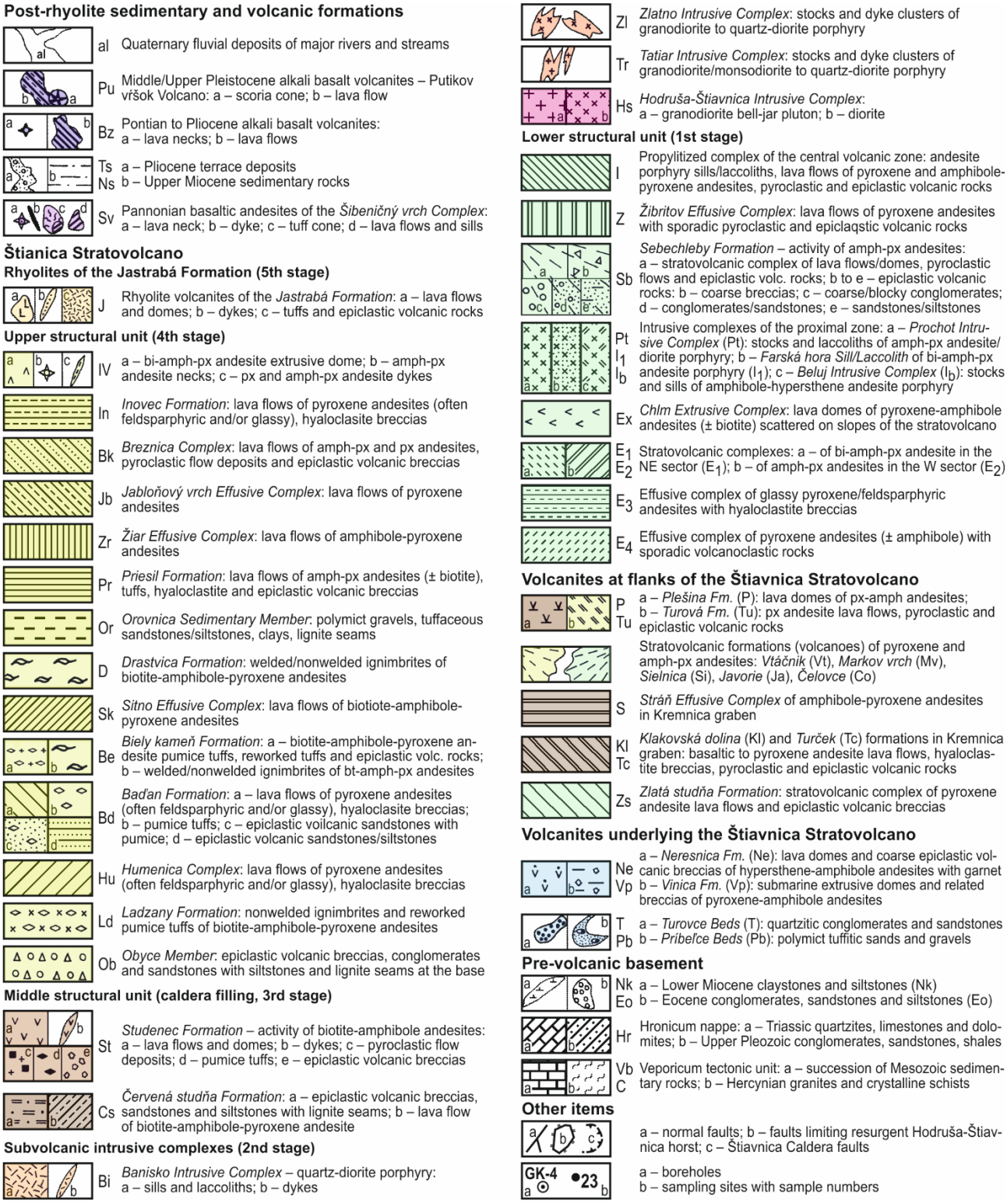


***Figure 1b.*** *Legend for the structural scheme (Fig. 1a).*

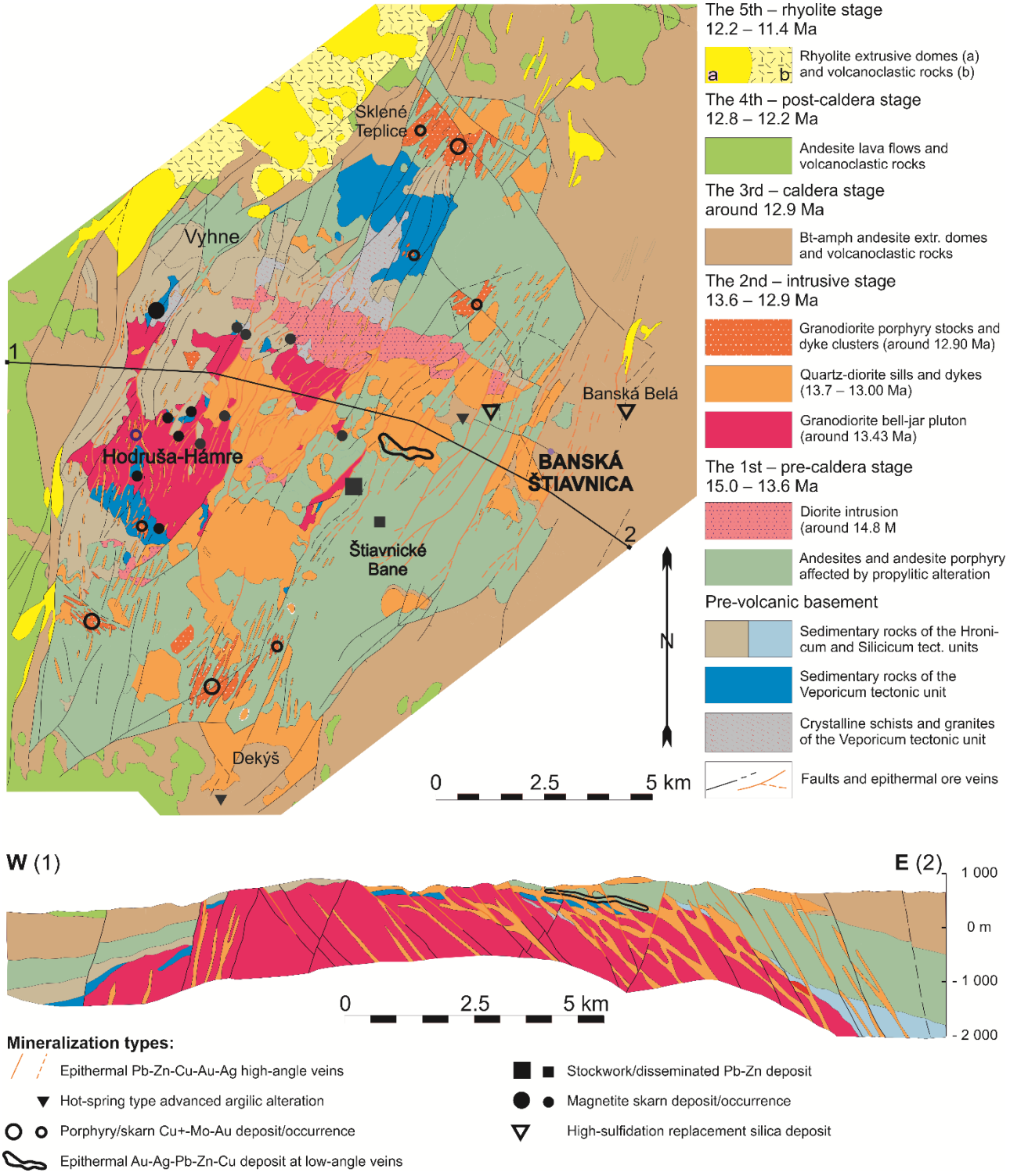


***Figure 2.*** *Structural scheme and section of the resurgent horst in the center of the Štiavnica Stratovolcano caldera with the location of main mineralization types. Modified after Lexa et al. (1999).*

In the central zone of the edifice, rocks of the pre-caldera stage are exposed in the eastern half of the resurgent horst (Figs. 1 and 2). Here, the former stratovolcanic edifice has been deeply eroded and is built mostly of andesite sills and laccoliths emplaced in the lower part of the edifice. The pre-caldera stage also comprises a stock of bt-amph-px diorite porphyry south of the caldera (~14.5 Ma, **stage 1b**) that hosts a sub-economic Beluj Au-porphyry mineralization.

During the **2nd stage** in the evolution of the Štiavnica Stratovolcano edifice (dated to the interval 13.6–12.9 Ma) a break in volcanic activity, extensive denudation in its central zone, and emplacement of subvolcanic/ intravolcanic intrusions took place. The subvolcanic/ intravolcanic intrusive complex is exposed in the uplifted block of the resurgent horst in the central zone of the

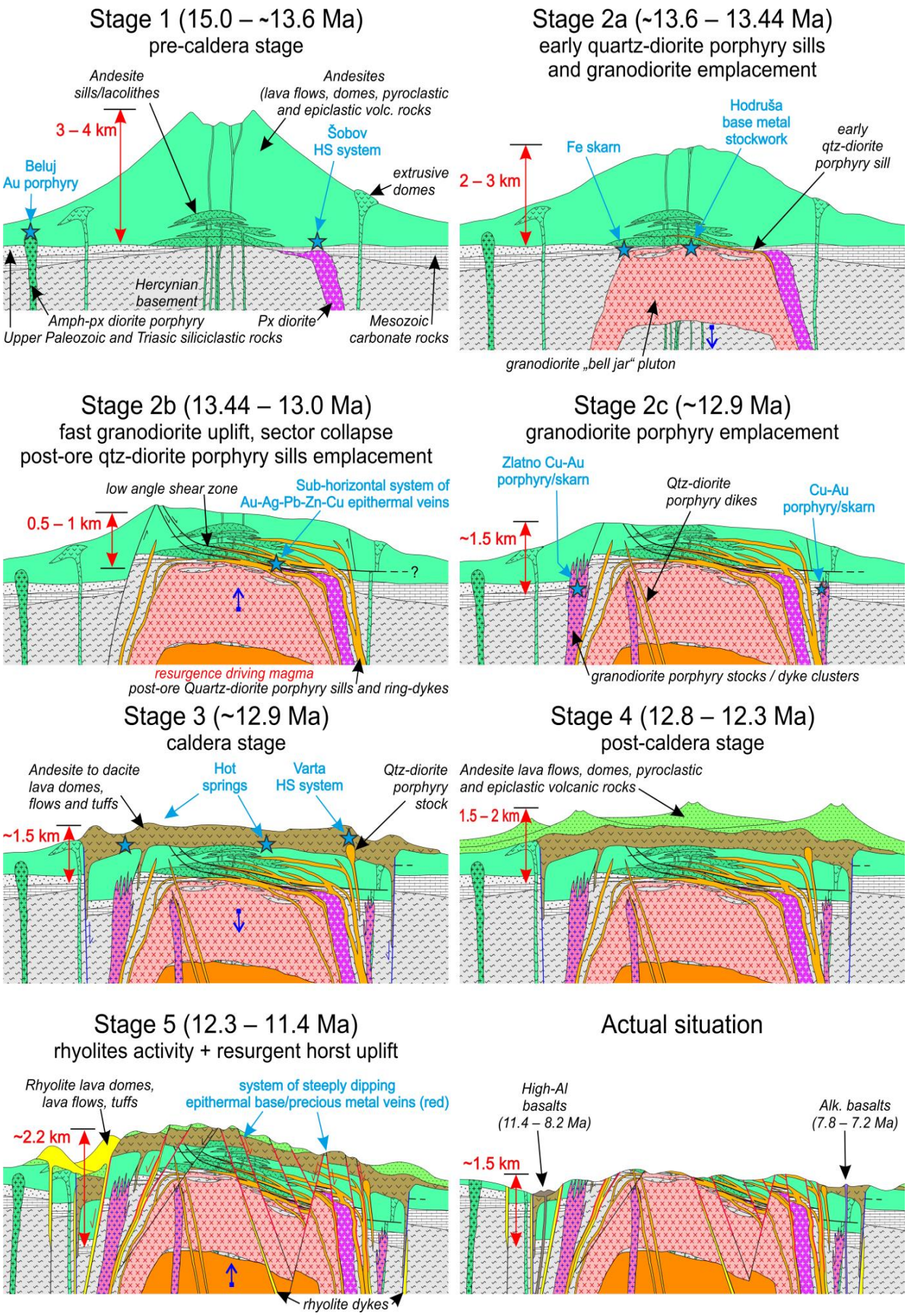


***Figure 3.*** *Evolution of the Štiavnica Stratovolcano edifice and associated mineralizations (Lexa et al. 2025).*

volcano (Figs. 1 and 2). The oldest diorite intrusion (~14.8 Ma) is the parental intrusion of the barren Šobov high-sulfidation hydrothermal system. A younger granodiorite bell-jar pluton (~13.44 Ma, **stage 2a**), emplaced by the underground cauldron subsidence mechanism, invaded basement rocks especially using subhorizontal discontinuities in the Mesozoic sedimentary formations above the Variscan crystalline rocks (Fig. 3). Three types of mineralizations are associated with the emplacement of the granodiorite bell-jar pluton. At contacts of the pluton with basement carbonate rocks there are magnetite skarn deposits and occurrences. In the central part of the pluton the overlying pre-caldera stage andesites are affected by extensive advanced argillic alteration, while underlying granodiorite and fragments of basement rocks host a stockwork-disseminated base metal mineralization.

Kubač et al. (2018) revealed that the extensive denudation was related to a resurgent uplift of the granodiorite pluton and associated sector collapse at the SE side of the edifice in the interval 13.44–13.3 Ma (Fig. 3). A basal, low angle detachment/ shear zone hosts the Hodruša precious/base metal epithermal mineralization.

Quartz-diorite porphyry sills (**stage 2b**) invaded major subhorizontal discontinuities in the basement, granodiorite pluton, contact of basement and volcanic complex and overlying andesites of the pre-caldera stage (Fig. 2). Sills emplaced among andesites occur especially in the area of the sector collapse where they intrude structures of the shear zone, both low angle faults as well as moderately dipping tension faults (Kubač et al., 2018). Emplacement of sills (13.3–13.0 Ma) post-dated the precious/base metal mineralization of the shear zone, with the exception of few thin sills parallel with the roof

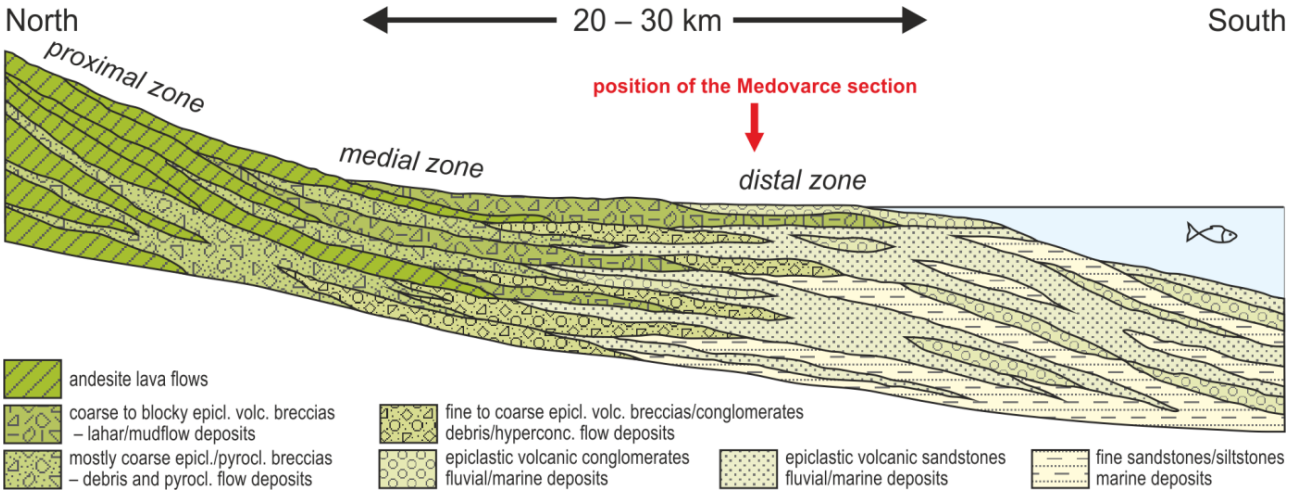


***Figure 4.*** *Facies model of the Sebechleby Formation.*

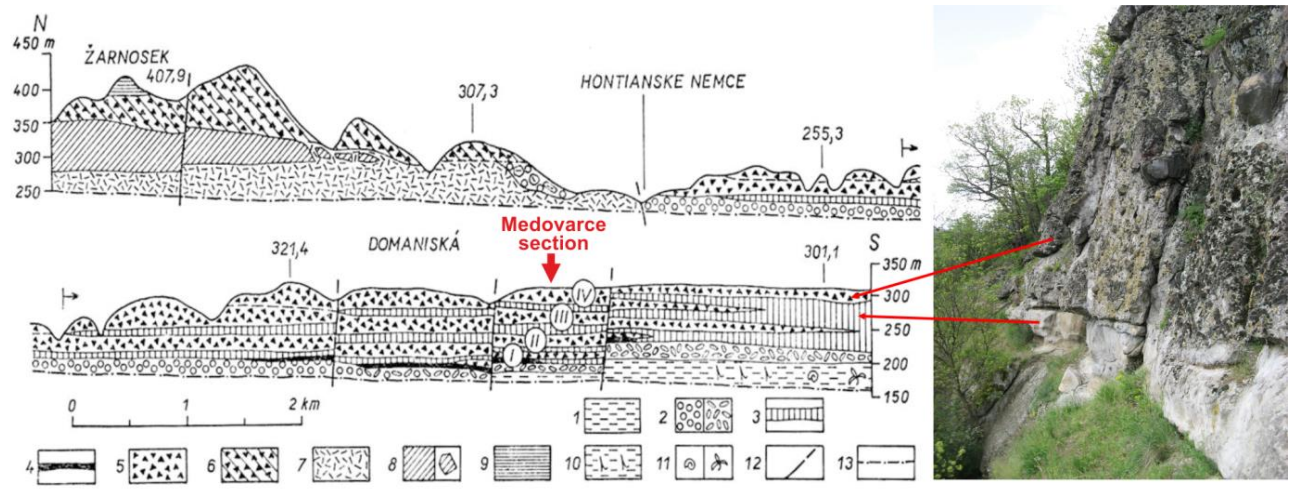


***Figure 5.*** *Section of the Sebechleby Fm. north and south of the locality Medovarce (Konečný 1966, photo Jaroslav Lexa). 1 – marine tuffaceous siltstones; 2 – coarse/fine conglomerates; 3 – fine to coarse sandstones; 4 – siltstones/claystones; 5 – coarse lahar breccias; 6 – mostly coarse epicl.volc. breccias; 7 – pumice flow deposits; 8 – amph-opx andesite lava flow; 9 – two px andesite lava flow; 10 – tree remnants; 11 – fauna and flora remnants; 12 – faults; 13 – base of the section.*

of the granodiorite that were emplaced before the mineralization and the granodiorite pluton emplacement (~13.60 Ma). Further eastward the sills pass into moderately outward dipping ring dikes.

Granodiorite to quartz-diorite porphyry dike clusters and small stocks (~12.9 Ma, **stage 2c**) are situated at the periphery of the granodiorite pluton (Figs. 2 and 3). Stocks with roof pendants in basement rocks pass upward into dike clusters emplaced in andesites of the pre-caldera stage. Intrusions of granodiorite porphyry are accompanied by the Cu-Au skarn-porphyry type mineralization.

Quartz-diorite porphyry dikes extend in the western and northern parts of the resurgent horst, outside of the sills extent. They are mostly thin, either vertical or dipping inward, showing some aspects of cone sheets. They post-date granodiorite porphyry stocks/dike clusters and quartz-diorite porphyry sills.

During the **3rd or caldera stage** (~12.9 Ma) subsidence of the Štiavnica caldera took place. Related volcanic activity filled the caldera and formed contemporaneous volcanic deposits on slopes of the Štiavnica Stratovolcano edifice (Figs. 2 and 3). The caldera has 20 km in diameter (Fig. 1) and the extent of its subsidence is estimated at 500 m. It is not of an explosive type, but it is filled by bt-amph andesite/dacite extrusive domes, dome flows and associated pyroclastic and epiclastic volcanic rocks. Tuffaceous sediments at the base of the caldera filling and underlying andesites of the pre-caldera stage are locally affected by advanced argillic alteration showing typical features of hot-spring type systems. Andesites of the caldera fill at its eastern part host a barren Varta high-sulfidation hydrothermal system with advanced argillic alteration.

During the **4th or post-caldera stage** (12.8–12.3 Ma) a renewed activity of less evolved andesites created explosive, stratovolcanic and effusive volcanic complexes/formations that rest upon caldera fill and outside of the caldera on slopes of the Štiavnica Stratovolcano edifice (Fig. 1). Individual complexes/ formations are spatially limited to certain sectors of the edifice. In the distal zone they pass into aprons of epiclastic volcanic breccias, conglomerates and sandstones.

During the **5th or late stage** (12.3–11.4 Ma) rhyolite volcanic activity created dikes, cryptodomes and extrusive domes on N S to NE-SW striking faults, including marginal faults of a contemporaneous resurgent horst in the central part of the caldera and local horsts west of the caldera (Figs. 1 and 2). An extensive dome/flow complex with related pyroclastic and epiclastic rocks spreads along southeastern and eastern marginal faults of the Žiar depression in the northern sector of the Štiavnica Stratovolcano edifice. Faults of the resurgent horsts host also an extensive system of intermediate to low-sulfidation precious/base metal epithermal veins. The hydrothermal system and rhyolite activity were contemporaneous.

An interested reader can find more details concerning structure and evolution of the Štiavnica Stratovolcano in the open access paper by Chernyshev et al. (2013). Timing of the evolution has been updated by Lexa et al. (2025). Abstract by Lexa & Koděra (this volume) provides essential information concerning magmatic and metallogenetic evolution of the stratovolcano (including references omitted from the text above). Magmatic evolution is in a greater detail treated in the paper by Rottier et al. (2000). Naturally, the mentioned papers include references to works with supporting evidences.

# 3. Field trip localities (their localization is in Fig. 1)

## *3.1. Medovarce – the 1st pre-caldera stage, Sebechleby Formation: succession of shallow marine epiclastic volcanic conglomerates/ sandstones and inter-bedded lahar deposits*

The Sebechleby Formation occupies a large area in the SE sector of the Štiavnica Stratovolcano (Fig. 1). While at the slopes of the stratovolcano (proximal zone) it is formed of extrusive domes, lava flows, pyroclastic flow deposits and coarse epiclastic volcanic breccias, in a shallow marine environment of the distal zone it is formed of epiclastic volcanic conglomerates, sandstones and lahar breccias that grade southward into succession of marine tuffaceous siltstones with inter-bedded horizons of submarine slide sandstones and conglomerates. In its distal zone the Sebechleby Fm. represents a coarse clastic delta prograding into a shallow marine environment of the Badenian sea (Fig. 4). Lahars (debris flows and mudflows) crossed a coastline and traveled quite far into the sea, where they rested on sorted sandstones and fine conglomerates of the beach and fore-beach environments (Fig. 5) and subsequently were reworked partially into horizons of coarse conglomerates (Fig. 4).

From the petrographic point of view the Sebechleby Formation includes material of amphibole-orthopyroxene andesites and two-pyroxene andesites with sporadic amphibole. Phenocrysts of plagioclase, clinopyroxene, orthopyroxene and brown amphibole rest in groundmass of hyalopilitic, microlitic or micropoikilitic texture (Fig. 6).

Locality Medovarce represents a type section of the Sebechleby Fm. sublitoral facies in the distal zone of the Štiavnica Stratovolcano (Figs. 4 and 5). Essential aspects of the section are demonstrated in the Fig. 7.

## *3.2. Ladzany – the 4th post-caldera stage, Baďan Formation: pyroxene andesite lava flow*

The Baďan Formation occupies a large area in the S and SW sector of the Štiavnica Stratovolcano (Fig. 1). It is a product of explosive and effusive activity of pyroxene andesites at the slope of the stratovolcano outside of the

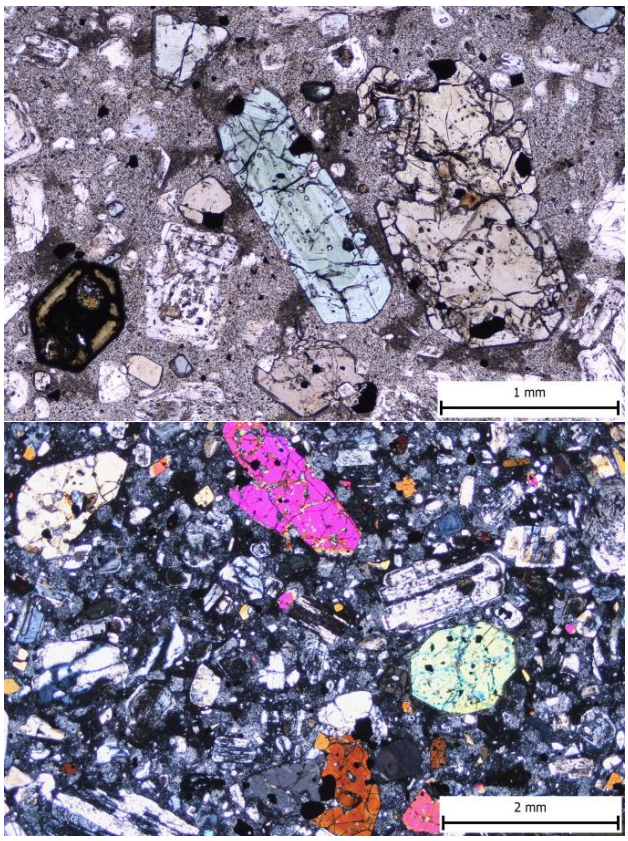


***Figure 6.*** *Microphoto of two-pyroxene andesite with sporadic amphibole. Top: II nicols, bottom: X nicols.*

caldera. Lava flows extend downward into coastal zone of the Early Sarmatian sea where they spread into a broad lava plateau extending over 80 km$^2$, with thickness 100–150 m. Individual flows show thickness 15–35 m. Disintegration at contacts with sea water created extensive zones of hyaloclastite breccias that were subsequently transformed into horizons of reworked hyaloclastite material. Breccias and conglomerates accumulated in the coastal zone next to the lava flows. Associated explosive activity, mostly of the vulcanian type, provided a large volume of pumice and ash that accumulated along with reworked sandy to gravely hyaloclastite material further southward in the litoral zone of the sea (locality Brhlovce).

From the petrographic point of view the Baďan Formation includes material of pyroxene andesites and feldspar-phyric andesites, often of a glassy nature. Phenocrysts of plagioclase, clinopyroxene and orthopyroxene rest in grondmass showing variably hyalopilitic, microlitic or piltaxitic texture.

In a small abandoned quarry at the Ladzany locality there is exposed interior of one of the andesite lava flows. Solidified massive lava shows a characteristic platy to blocky jointing respecting planes of incipient lamination that imply lava cooling during movement. In the central part of the quarry it is subhorizontal, parallel with the base of the lava flow (Fig. 8a). At the left side of the quarry orientation of the platy jointing turns gradually to almost vertical one, indicating a marginal part of the lava flow. Here a strike of jointing is parallel with the flow direction. The flow direction is also indicated by pronounced striations on a vertical discontinuity in the central part of the quarry that accommodated a differential movement of the flow portions (Fig. 8b).

### *3.3 Brhlovce – the 4$^{th}$ post-caldera stage, Baďan Formation: succession of shallow marine reworked pumice tuffs, pumiceous sandstones and epiclastic volcanic sandstones*

For a general description of the Baďan Formation see the locality Ladzany above. South of the extensive lava plateau and related hyaloclastite breccias it is represented by accumulations of reworked pumiceous/tuffaceous and hyaloclastite material transported and deposited in a litoral environment of the Early Sarmatian sea (Fig. 1). At the north pumice tuffs and tuffs dominate over intercalations of reworked dark sandy to gravely glassy andesite material (locality Brhlovce), while further southward epiclastic volcanic sandstones, variably with pumice admixture, dominate over intercalations of pumiceous and/or tuffaceous material. At the south the formation is formed mostly of tuffaceous sandstones and siltstones.

At the abandoned quarry next to the village Brhlovce (Fig. 9) there is exposed a succession of reworked pumice tuffs interbedded with epiclastic volcanic sandstones. Thick poorly sorted beds of pumice tuffs alternate with layers of moderately sorted pumice bearing sandstones and well sorted and laminated epiclastic volcanic sandstones. While nature of pumice fragments implies the vulcanian and/or subplinian types of eruptions as the source of primary deposits, glassy nature of sandstones grains implies as their source hyaloclastite breccias and lava flows north of the locality. Rounding of pumice fragments and sandstone grains corresponds to reworking in a coastal zone of the sea. Bench-like beds of poorly sorted material were transported as gravity driven density flows. Laminated layers of sorted material point to a traction transport and deposition driven by currents.

### *3.4. Počúvadlo – the 4$^{th}$ post-caldera stage, Biely kameň Formation: welded ignimbrite of biotite-amphibole-orthopyroxene andesite*

The Biely kameň Formation represents pyroclastic deposits of one of the andesite explosive events during the post-caldera stage that alternate with periods of andesite effusive activity. It followed activity of the Baďan formation pyroxene andesites and preceded activity of the Sitno Effusive Complex biotite-amphibole-orthopyroxene andesites (Fig. 1b). A thicker accumulation of pumice tuffs (including welded ignimbrite at the Počúvadlo locality), reworked pumiceous tuffs and pumice bearing epiclastic volcanic sandstones and/or fine breccias extends in the southern part of the caldera

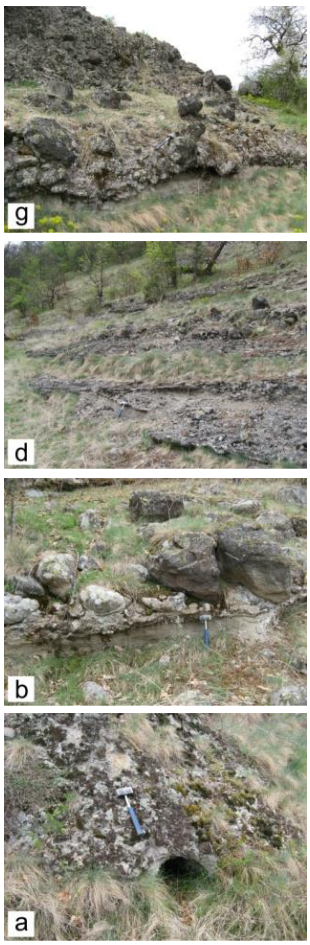


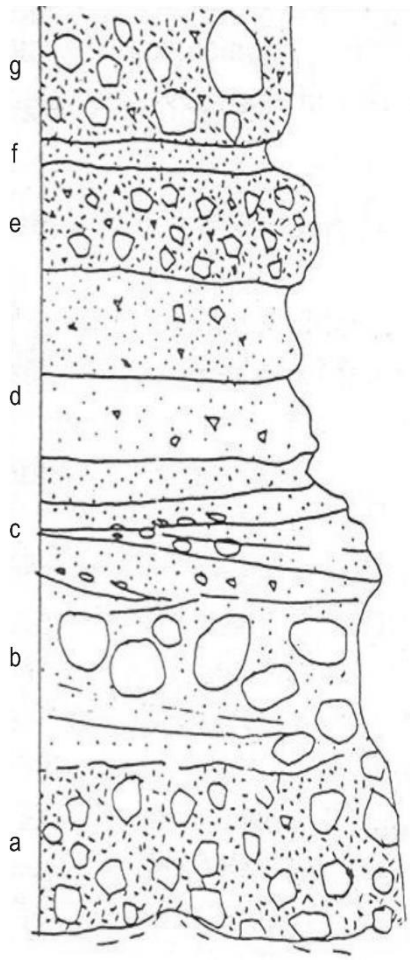


*g – Very coarse chaotic lahar breccia with andesite blocks up to 2 m in diameter; compact tuffaceous matrix with porous andesite fragments points to deposition in a hot state.*

*f – Reworked tuff with dispersed pumice implies a contemporaneous explosive activity.*

*e – Chaotic lahar breccia with andesite blocks up to 0.5 m in diameter.*

*d – Alternation of poorly sorted sandstones and unsorted fine breccias implying transport and deposition by hyperconcentrated debris flows.*

*c – Mostly coarse, stratified sandstones including andesite fragments/pebbles and irregular gravel lenses – fluvial and/or hyperconcentrated flow deposits.*

*b – Coarse to blocky conglomerates with sandstone intercalations, coastal marine deposits.*

*a – Chaotic lahar breccia with andesite blocks up to 1 m in diameter; tuffaceous sandy matrix includes a silt/clay component implying a transition towards a mudflow type transport and deposition; a big hole is after an enclosed tree trunk.*

***Figure 7.*** *Lithologic column of the Sebechleby Formation at the locality Medovarce. Drawing by V. Konečný.*

***Figure 8a.*** *Pyroxene andesite lava flow showing platty to blocky jointing in its internal part.*

***Figure 8b.*** *Striations on a vertical discontinuity in the central part of the quarry that accommodated a differential movement of the flow portions.*

(Fig. 1). Elsewhere in the caldera and on slopes of the stratovolcano the formation is represented by generally thin horizons of reworked pumiceous tufs, epiclastic volcanic sandstones and rare siltstones at the base of the Sitno Effusive complex lava flows.

At the locality Počúvadlo there is exposed a thicker horizon of welded pumice flow deposits – ignimbrite. As demonstrated in the Fig. 10a, it grades downward into unwelded pumice flow deposits, that rest on a thin horizon of reworked pumiceous tuffs and an older lava flow of the Baďan Formation (not exposed at the locality). Welded ignimbrite shows a typical compaction and contraction columnar jointing (Fig. 10b) due to a pumice flow deposition at the high temperature. Former pumice fragments are flattened into lenses of gray glass that are known as fiamme (Fig. 10c). Microphoto (Fig. 10d) shows

***Figure 9a.*** *Succession of reworked pumice tuffs and epiclastic volcanic sandstones in the village.*

***Figure 9b.*** *Detail of larger pumice fragments in poorly sorted pumice tuff. Dark color indicates andesitic compositon (smaller pumices are bleached).*

***Figure 9c.*** *A thick unsorted pumice tuff bed grades upward into a tuffaceous silt. That implies transport by a density current.*

***Figure 9d.*** *An eroded channel is filled by sorted pumice.*

***Figure 9e.*** *Mixed facies of pumice and sandy andesitic material. With an exception of a mixed layer of pumice and sand sorting, lamination and inclined layers imply a traction transport.*

***Figure 9f.*** *Detail of the mixed layer of pumice and sand. Thanks to a low-density large pumice fragments show the same transport dynamics as andesite sand grains.*

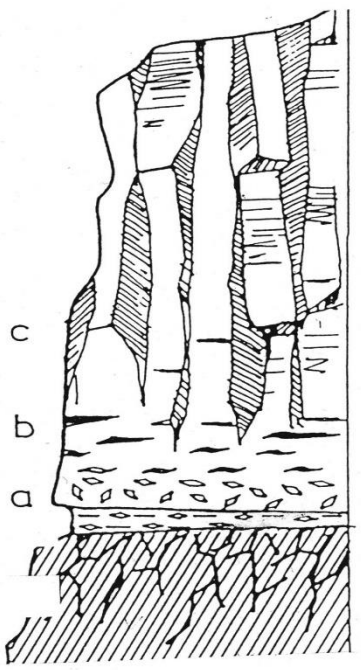


***Figure 10a.*** *A section of the ignimbrite horizon, lower parts are not exposed. Explanation is in the text. Drawing by V. Konečný).*

***Figure 10b.*** *Exposed part of the ignimbrite showing a typical columnar jointing.*

***Figure 10c.*** *A detail of ignimbrite with fiamme – flattened pumice fragments.*

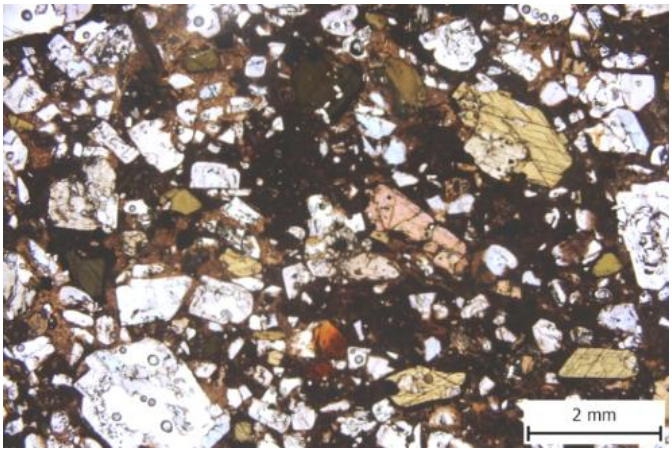


***Figure 10d.*** *Microphoto of welded ignimbrite. Note porous brownish glass of pumice fragments.*

phenocrysts of plagioclase, orthopyroxene, amphibole and sporadic biotite in brownish porous glass of deformed pumice fragments.

### *3.5. Šementlov – the 2nd stage of subvolcanic intrusions, Zlatno Intrusive Complex: granodiorite porphyry stock/dike showing a porphyry system quartz-sericite-pyrite alteration*

The Zlatno Intrusive Complex comprises granodiorite to rare quartz-diorite porphyry dike clusters and small stocks situated at the periphery of the granodiorite pluton (Figs. 1 and 2). In andesites of the post-caldera stage porphyry intrusions appear as dike clusters (Fig. 11). At basement level, they pass into stock-like bodies with numerous engulfed blocks of surrounding rocks. Only at great depth do porphyry intrusions pass into massive bodies without enclosed basement blocks. The extent of dike clusters is up to 2–3 km$^2$ at the surface; however, sections of granodiorite porphyry stocks at deeper levels do not exceed 1 km$^2$. Intrusions are formed by phenocryst rich biotite–amphibole granodiorite porphyry (Fig. 12a, e and f) and rare quartz–diorite porphyry (Fig. 12b). All phenocrysts show resorption prior onset of groundmass crystallisation. Accessories include magnetite, ilmenite, apatite and zircon. Groundmass shows mostly microallotriomorphic-granular texture (Fig. 12f). It consists of hypidiomorphic biotite, anhedral quartz and orthoclase, rare amphibole and Fe–Ti oxides. With increasing depth, granodiorite porphyry pass into porphyritic granodiorite (Fig. 12c). A mutual relationship

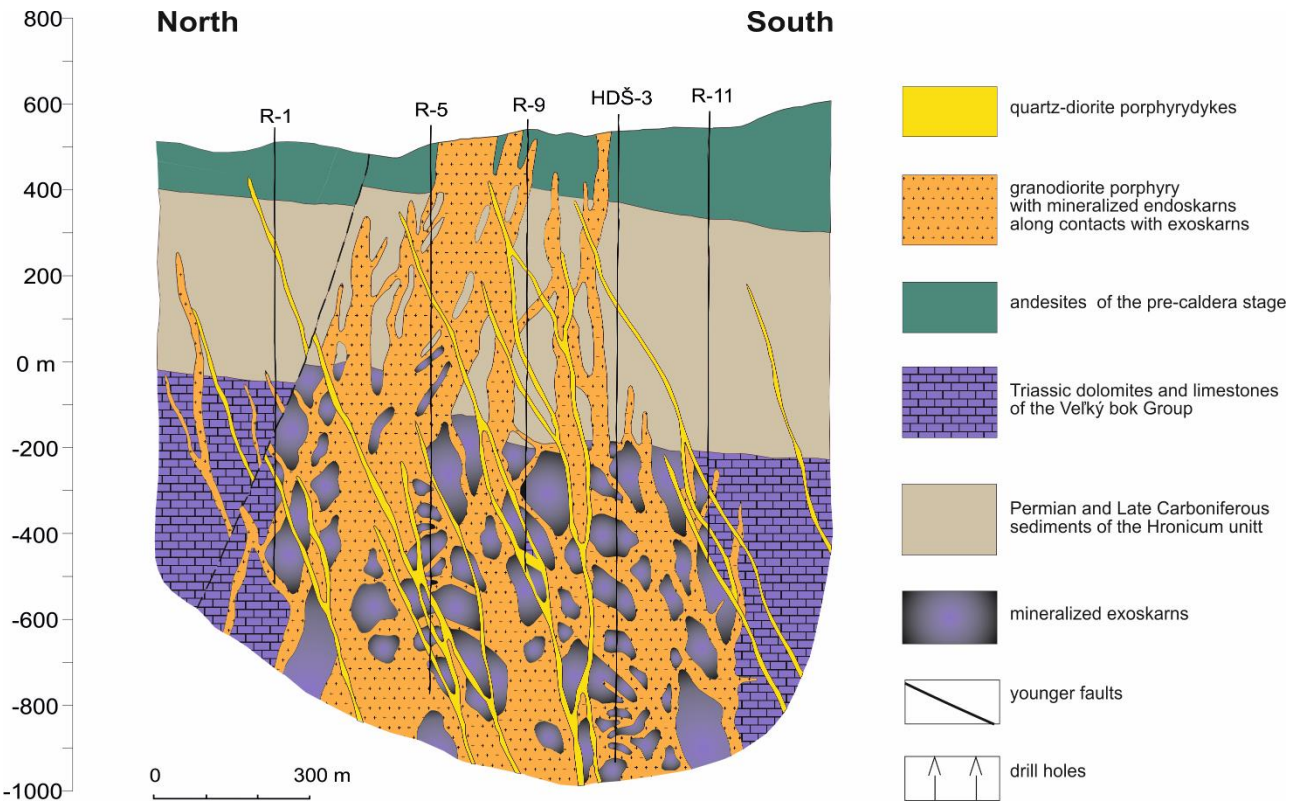


***Figure 11.*** *Section of a granodiorite porphyry stock/dike cluster at the Zlatno locality (Lexa, 1977).*

of petrographic types indicates multiple intrusions from a differented magma chamber. Sporadic mafic enclaves (Fig. 12d) imply a role of magma reservoir recharge in the intrusions emplacement. Magma recharge and mixing is indicated also by plagioclase grains that show resorbed An-poorer cores with patches of An-rich plagioclase in a sieve texture, surrounded by an An-rich zone as well as tiny iclusions of orthopyroxene, amphibole and biotite in their resorbed cores.

Intrusions of granodiorite porphyry are accompanied by the Cu-Au skarn-porphyry type mineralization, with granodiorite porphyry stocks as centres of alteration zoning. An internal K-silicate zone (K-feldspar, secondary biotite), overlaps in depth with Ca–Na zone (actinolite) and is surrounded by the phyllic zone (quartz, sericite, pyrite). In upper parts of the systems, a discontinuous zone of argillic alteration occurs (illite, kaolinite, pyrophyllite, smectite). The most external zone is represented by propylitic alteration (chlorite, carbonate).

At the Šementlov locality we have a chance to observe relatively fresh blocks of granodiorite porphyry and blocks affected partially by a quartz-sericite-pyrite alteration of the Šementlov porphyry system phyllic zone. The porphyry shows a coarse porphyritic texture with phenocrysts of plagioclase, amphibole and biotite in groundmass of microaplitic texture (Fig. 13).

### *3.6. Hodruša – Mayer shaft – the 2nd stage of subvolcanic intrusions, Hodruša-Štiavnica intrusive complex: top of the granodiorite bell-jar pluton*

The granodiorite bell-jar pluton is exposed in the central part of the resurgent horst (Figs. 1 and 2). Including covered parts it extends over the area 100 km$^2$. The pluton of an elliptical shape has an almost flat top and outward dipping margins (Fig. 2). Its thickness exceeds 2,500 m. For the emplacement it has used subhorizontal discontinuities in the Mesozoic sedimentary formations above the Variscan crystalline rocks and bellow volcanic formations (Figs. 2 and 14). Apparently, it was emplaced by the underground cauldron subsidence mechanism – a thick conical block of basement rocks subsided into the upper part of magma reservoir and magma of a lesser density filled gradually the increasing gap, forming the bell-jar pluton (Fig. 3, stage 2a). This mechanism of the emplacement is confirmed by the presence of flat roof pendants as well as by magnetic anisotropy measurements (Tomek et al. 2014) close to the roof of the pluton indicating the initial stage of the emplacement in the form of a sill.

Granodiorite is pale, coarse-grained magmatic rock mostly with equigranular, at margins with porphyritic hipidiomorphic-granular texture (Fig. 15). It consists of intermediate plagioclase, amphibole, biotite and magnetite in hypidiomorphic forms, mostly 2–5 mm in diameter (50–60 %), whereas quartz and orthoclase form anhedral, often poikilitic grains in the case of the

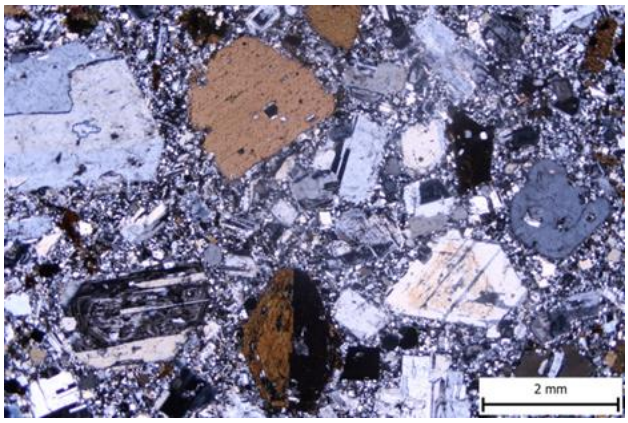


***Figure 12a.*** *Microphoto of granodiorite porphyry with phenocrysts of plagioclase, amphibole and biotite in micro-aplitic groundmass, locality Zlatno.*

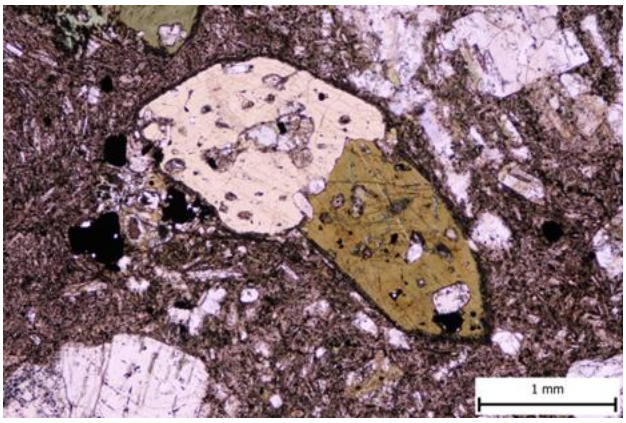


***Figure 12b.*** *Microphoto of quartz-diorite porphyry with phenocrysts of plagioclase, amphibole and biotite in micro-hipidiomorphic-granular groundmass, locality Zlatno.*

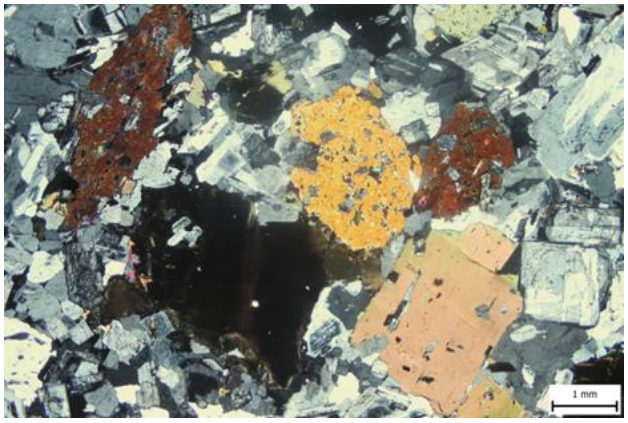


***Figure 12c.*** *Microphoto of porphyritic biotite-amphibole granodiorite with a coarse-grained aplitic groundmass, locality Zlatno, depth 1,500 m.í*

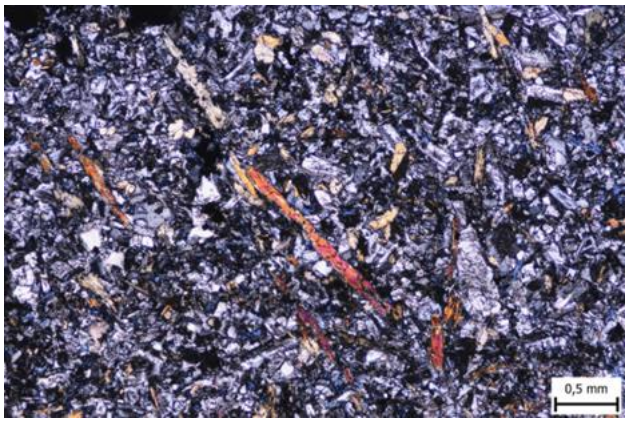


***Figure 12d.*** *Microphoto of a mafic enclave in granodiorite porphyry showing acicular amphibole crystals that imply crystallization at undercooling.*

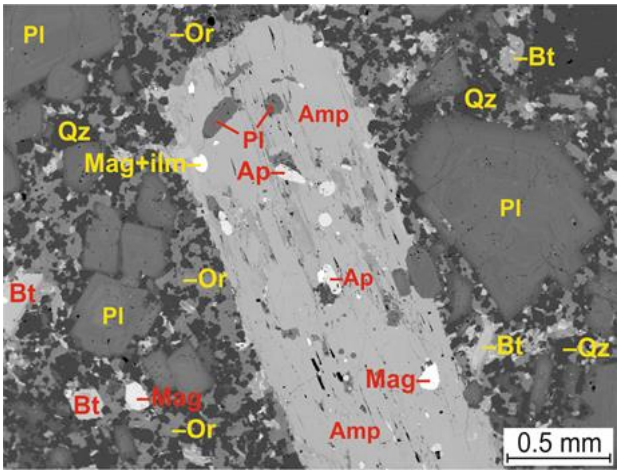


***Figure 12e.*** *BSE image of granodiorite porphyry – a phenocryst of amphibole with enclosed plagioclase, magnetite, ilmenite and apatite.*

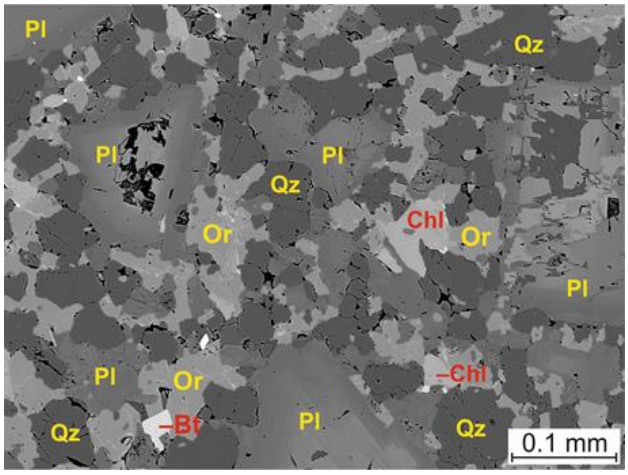


***Figure 12f.*** *BSE image of granodiorite porphyry – a detail of microallotriomorphic-granular groundmass.*

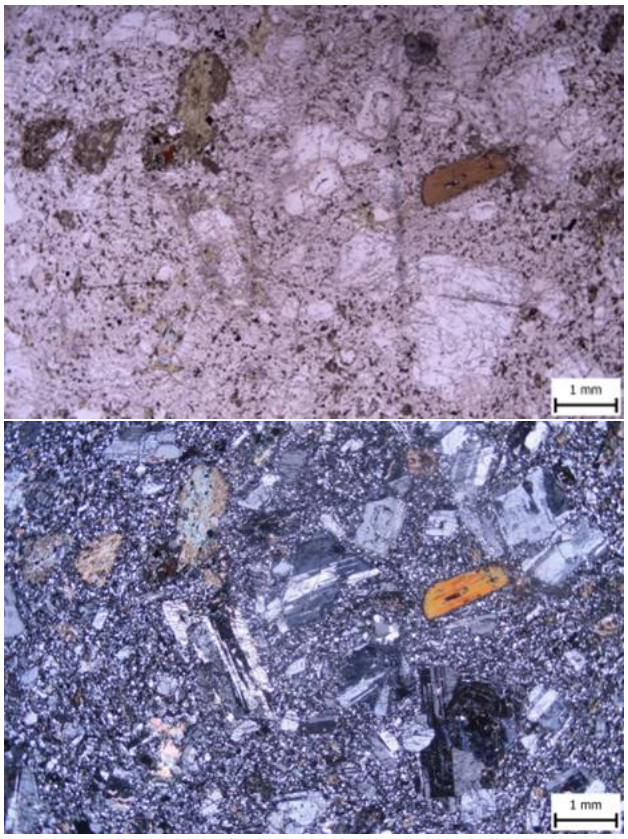


***Figure 13.*** *Microphotos of granodiorite porphyry from the Šementlov locality. Amphibole is replaced by chlorite and carbonate, plagioclase is partially replaced by sericite. Groundmass shows a microaplitic texture. Top: II nicols, bottom: X nicols.*

equigranular texture (Fig. 15a–d) or smaller anhedral groundmass grains, mostly 0.1–0.4 mm in diameter, in the case of the porphyritic texture Fig.15e–f). Idiomorphic amphibole and biotite grains were resorbed before a late stage eutectic crystalization of quartz, K-feldspar and Ab-rich plagioclase took place. Accessories include magnetite, ilmenite, apatite and zircon.

Idiomorphic to hipidiomorphic plagioclase is prismatic, variably intergrown with amphibole and biotite, at edges with late stage quartz and othoclase. Plagioclase magmatic zonality is not uniform. Mostly the An-richer core is surrounded by oscilatory zoning, grading repeatedly from An-richer zones to An-poorer zones. At margins there is a broader zone grading to An-poor composition at the edge. A part of plagioclase grains shows resorbed An-poorer cores with patches of An-rich plagioclase in a sieve texture, surrounded by an An-rich zone (evidence of magma mixing). Plagioclase grains include frequently tiny grains of magnetite, ilmenite, apatite and zircon, in the case of resorbed cores also biotite and amphibole.

Idiomorphic to hipidiomorphic amphibole grains are variably intergrown with and/or enclose smaller idiomorphic grains of plagioclase, biotite and magnetite. Magnetite, ilmenite, apatite and zircon are present also as tiny inclusions. Amphibole grains do not show any obvious zonality. However, they show a late stage replcement by amphibole richer in $SiO_2$ and MgO and poorer in $TiO_2$, $Al_2O_3$ and FeO.

Idiomorphic to hipidiomorphic biotite grains are variably intergrown with plagioclase and amphibole and enclose smaller idiomorphic grains of plagioclase and magnetite. Magnetite, ilmenite, apatite and zircon are

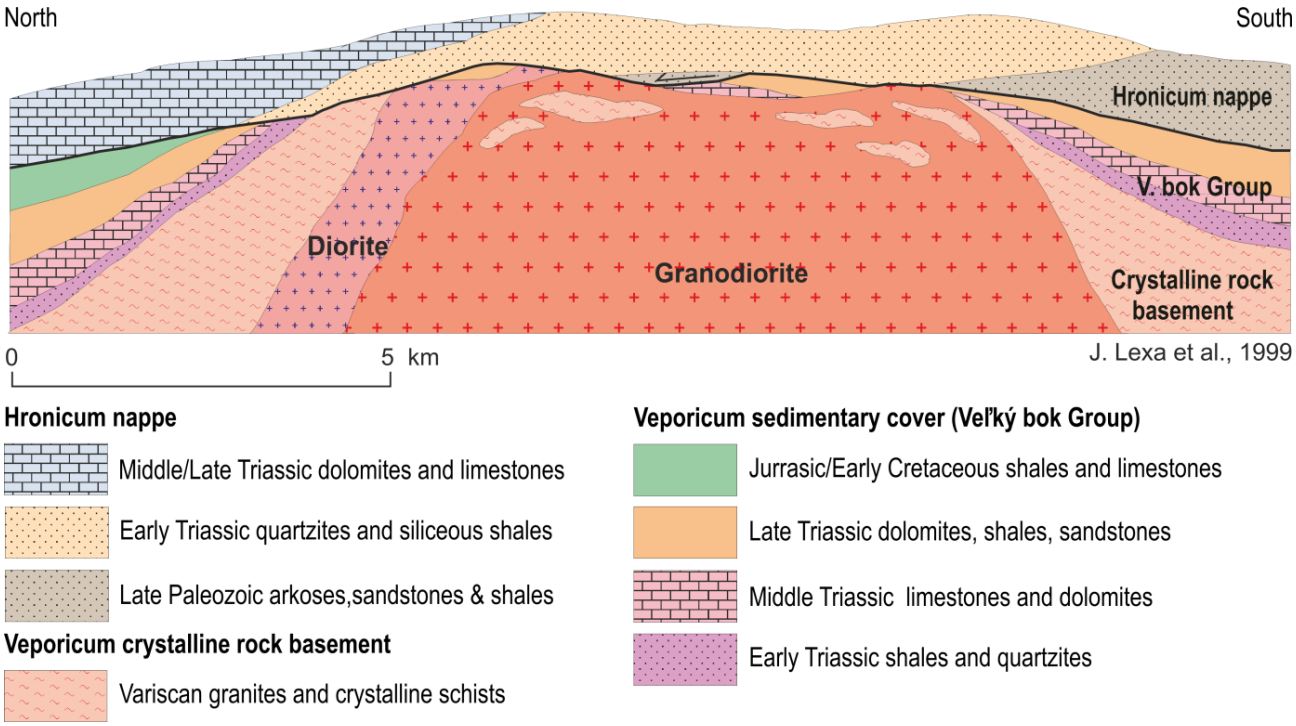


***Figure 14.*** *Structural relationship of the granodiorite bell-jar pluton and basement rocks.*

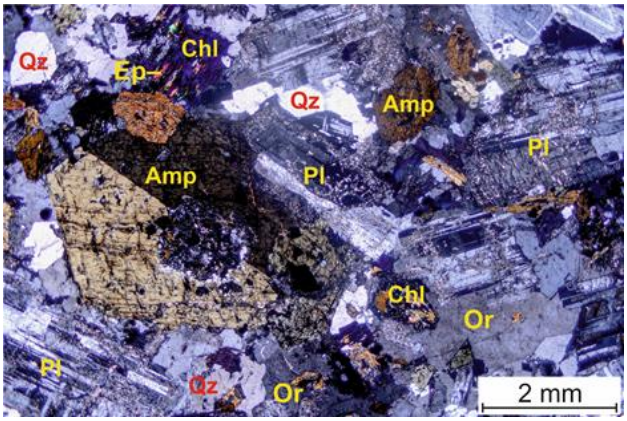


***Figure 15a.***

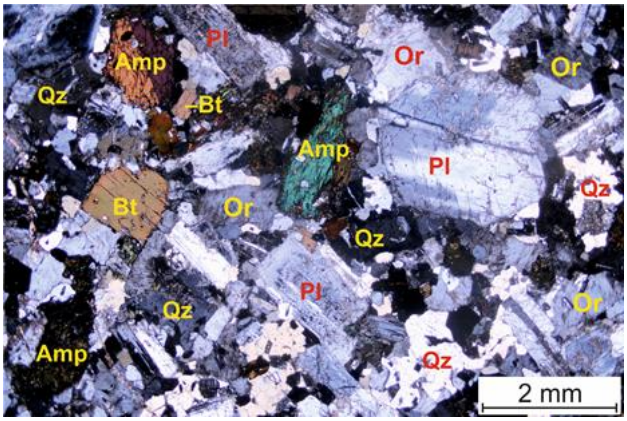


***Figure 15b.***

*Microphotographs of granodiorite (cross polarized light) showing coarse hipidiomorphic-granular texture with hipidiomorphic grains of plagioclase, amphibole and biotite (replaced by chlorite) and anhedral, partially poikilitic grains of quartz and orthoclase.*

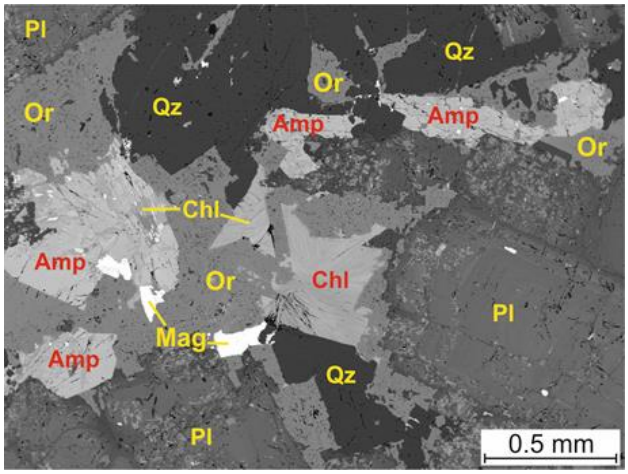


***Figure 15c.***

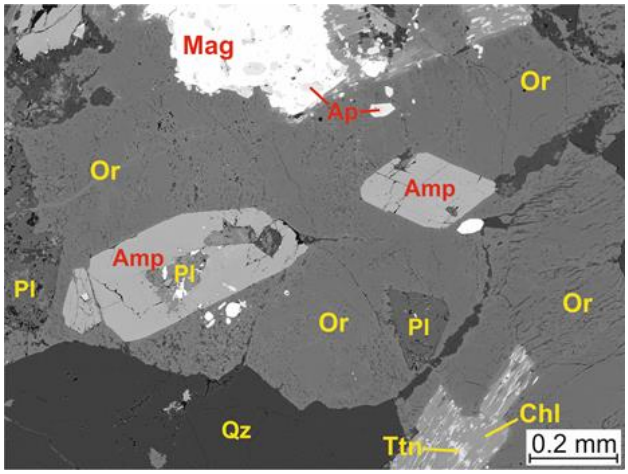


***Figure 15d.***

*BSE images of granodiorite demonstrate a poikilitic nature of the late stage quartz and orthoclase anhedral grains. Note tiny apatite inclusions in magnetite on Fig. 15c.*

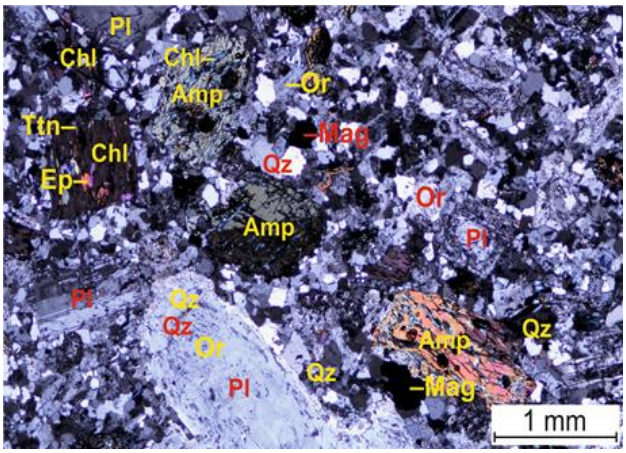


***Figure 15e.***

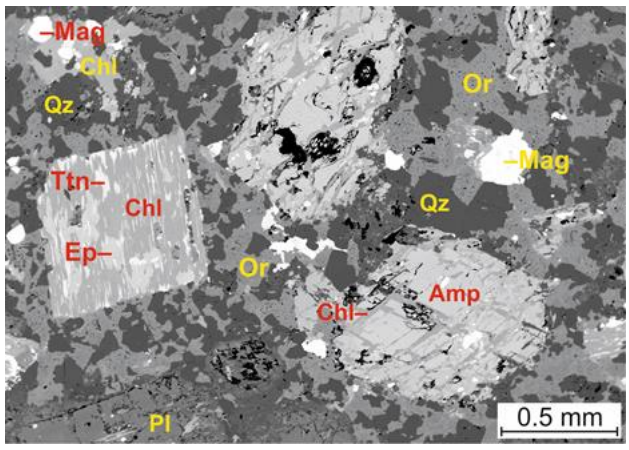


***Figure 15f.***

*Microphoto in cross-polarized light (Fig. 15e) and BSE image (Fig. 15f) of granodiorite from the marginal part of the pluton showing porphyritic texture.*

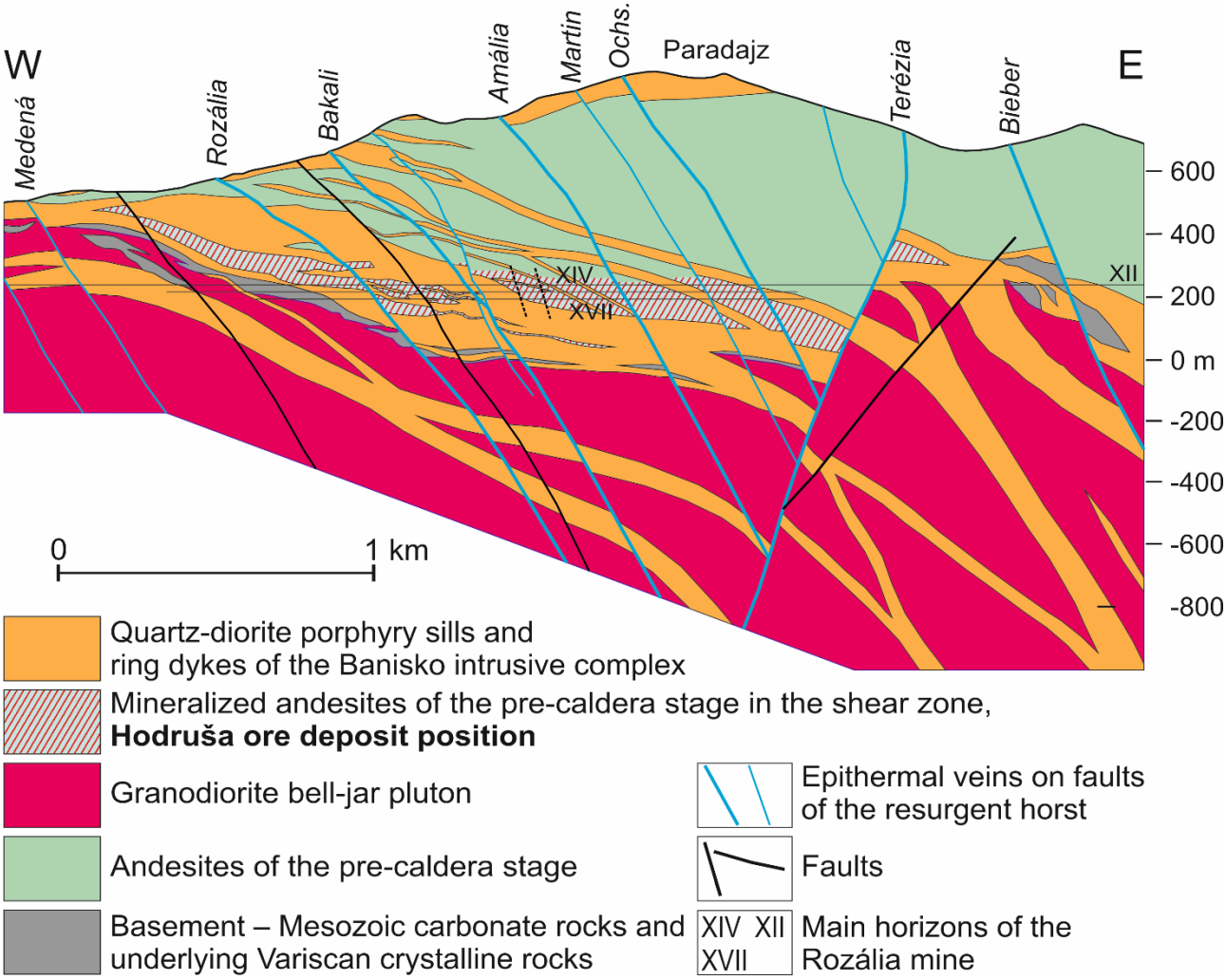


***Figure 16.*** *A section showing quartz-diorite porphyry sills in the area of the Hodruša precious/base metal ore deposit that pass eastward into outward dipping ring dikes (Kubač et al. 2018).*

present as tiny inclusions. Biotite is often replaced by chlorite, titanite and rare epidote.

Idiomorphic to hipidiomorphic magnetite and ilmenite grains occur mostly along edges of amphibole and biotite grains. Both are affected by lower temperature re-equilibration. Magnetite shows exsolution of ilmenite lamellae, while ilmenite shows exsolution of rutile.

Anhedral quartz and orthoclase grains (along with Ab-rich edges of plagioclase grains) represent a product of the late stage eutectic crystallization following emplacement of the granodiorite pluton. Their grain size is variable. At the internal parts of the pluton it exceeds the size of plagioclase, amphibole and biotite grains and shows a poikillitic texture. At margins of the pluton it is much smaller and granodiorite shows a porphyritic texture.

### *3.7. Hodruša – tajch – the 2nd stage of subvolcanic intrusions, Banisko Intrusive Complex: bt-amph quartz-diorite porphyry sill*

The Banisko Intrusive Complex comprises quartz-diorite porphyry sills of the resurgent horst (Figs. 1 and 2). Sills were emplaced along the top of the granodiorite pluton as well as in the upper part of the pluton and the lowermost part of the pre-caldera stage andesites (Fig. 16). Their thickness varies from few meters to a maximum of 200 m in the case of the sill at the top of the granodiorite pluton. In the broader surroundings of the Hodruša precious/base metal deposits sills intruded especially structures of a shear zone at the base of the sector collapse (Fig. 3 stage 2b and Fig. 16). Further eastward the sills pass into outward dipping ring dikes (Figs. 16 and 17). As in the case of the granodiorite bell-jar pluton sills and ring-dikes of the Banisko Intrusive Complex were emplaced by the underground cauldron subsidence mechanism (Fig. 17).

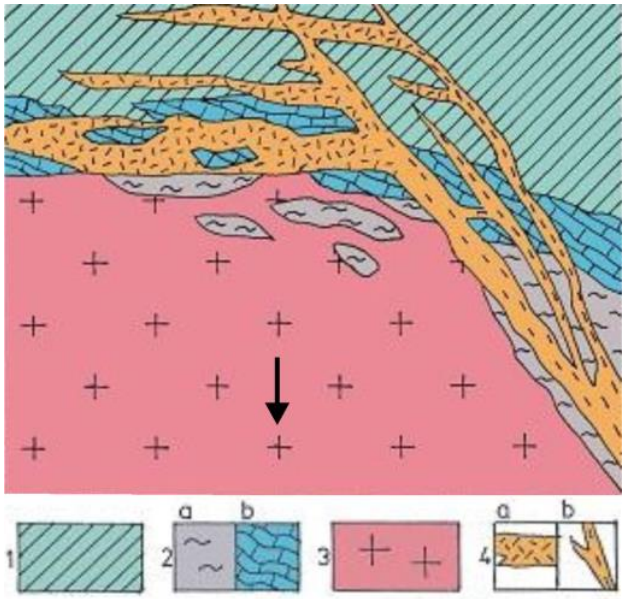


***Figure 17.*** *A section showing quartz-diorite porphyry sills in the area of the Hodruša precious/base metal ore deposit that pass eastward into outward dipping ring dikes (Kubač et al. 2018) Legend: 1 – Pre-caldera stage andesites, 2a – Crystalline rocks basement, 2b – Mesozoic sedimentary rocks, 3 – Granodiorite, 4a – Quartz-diorite porphyry sills, 4b – Quartz-diorite porphyry ring dikes.*

Quartz-diorite porphyry sills show a petrographic variability as far as the phenocryst assemblage, size and content are concerned and in groundmass textures. All of them contain phenocrysts of plagioclase, amphibole and biotite, some of them also phenocrysts of quartz. Based on these aspects we distinguish formally 4 essential types of quartz-diorite porphyry. However, in reality there exist also less frequent transitional types.

Coarse-grained quartz-diorite porphyry with quartz contain also resorbed quartz phenocrysts (Fig. 18a and b). Size of phenocrysts varies in the range 1–4 mm, rarely up to 5 mm, quartz phenocrysts do not exceed the size of 3 mm. The phenocryst content is 40–50 %. Microallotriomorphic-granular groundmass is composed of quartz and orthoclase.

Coarse-grained quartz-diorite porphyry without quartz contain only rare small resorbed quartz phenocrysts Fig. 18c and d). Size of phenocrysts varies in the range 1–3 mm, rarely up to 4 mm, rare quartz phenocrysts do not exceed the size of 0.5 mm. The phenocryst content is 40–50 %. Microallotriomorphic-granular groundmass is composed of quartz, orthoclase and minor An-poor plagioclase.

Medium-grained quartz-diorite porphyry with quartz contain also resorbed quartz phenocrysts (Fig. 18e and f). Size of phenocrysts varies mostly in the range 1–2.5 mm, rarely up to 3.5 mm, quartz phenocrysts do not exceed the size of 2 mm. The phenocryst content is 30–40 %. Fine microallotriomorphic-granular groundmass is composed of quartz and orthoclase.

Medium-grained quartz-diorite porphyry without quartz contain only very rare small resorbed quartz phenocrysts (Fig. 18d). Size of phenocrysts varies in the range 1–2.5 mm, rarely up to 3.5 mm, rare quartz phenocrysts do not exceed the size of 0.3 mm. The phenocryst content is 30–35 %. Fine microallotriomorphic-granular groundmass is composed of quartz, orthoclase and minor An-poor plagioclase.

Phenocrysts of quartz-diorite porphyry sills are mostly altered. If unaltered, plagioclase phenocrysts show a magmatic zonality with An-rich core surrounded by oscilatory zoning and a thin or no An-poor rim. Some of the phenocrysts show cores of lower An content – in such the case they are resorbed and replaced by plagioclase of higher An content in patchy texture (evidence of magma mixing). Amphibole and biotite phenocrysts enclose plagioclase and tiny grains of magnetite, ilmenite, apatite and rare zircon. Quartz-diorite porphyry are affected generally by propylitic alteration related to younger epithermal veins. Plagioclase is variably replaced by albite, sericite and carbonate, amphibole is replaced by carbonate, chlorite, epidote and magnetite and biotite is replaced by chlorite, epidote and magnetite.

At the locality Hodruša – tajch there is exposed at the surface a quartz-diorite porphyry sill that was emplaced above mineralized andesites of the Hodruša ore deposit (Fig. 16). It is massive, showing an irregular blocky jointing. The porphyry is coarse-grained with phenocrysts of plagioclase, amphibole and biotite in groundmass of the microallotriomorphic-granular texture (Fig. 18c and d). It is affected by propylitic alteration.

### *3.8. Juraj adit – the 2nd stage of subvolcanic intrusions, Banisko Intrusive Complex: bt-amph quartz-diorite porphyry ring dike*

For a general description of the Banisko Intrusive Complex see the locality Hodruša – tajch above.

A ring-dike exposed in the quarry at the locality Juraj adit is 120 m thick. It dips eastward at the angle of 60°. A geological position of the ring-dike is expressed by the eastern side of Fig. 16, while the mode of its emplacement by the underground cauldron subsidence mechanism is illustrated by Fig. 17. The exposed ring-dike has been emplaced into andesites of the pre-caldera stage. The quartz-diorite porphyry is massive, showing a blocky jointing that respects partially inclination of the ring-dike (Fig. 19a). It is coarse-grained (Fig. 19b) with phenocrysts of plagioclase, amphibole, biotite and quartz in fine microallotriomorphic-granular groundmass (Fig. 19c) composed of quartz and K-feldspar (Fig. 19d). Phenocrysts of quartz are rounded by resorption and some of them show a compositional zonality (Fig. 19d).

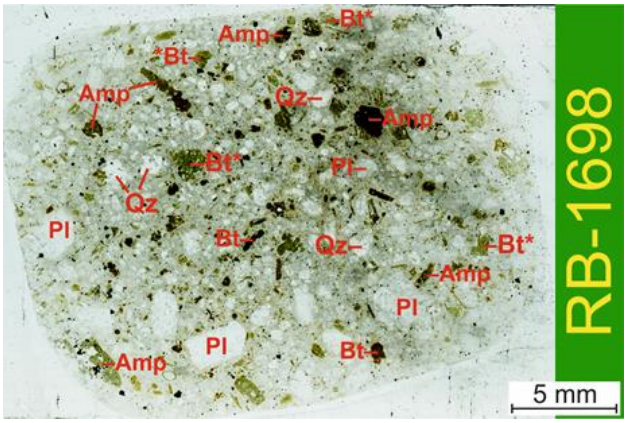


***Figure 18a.***

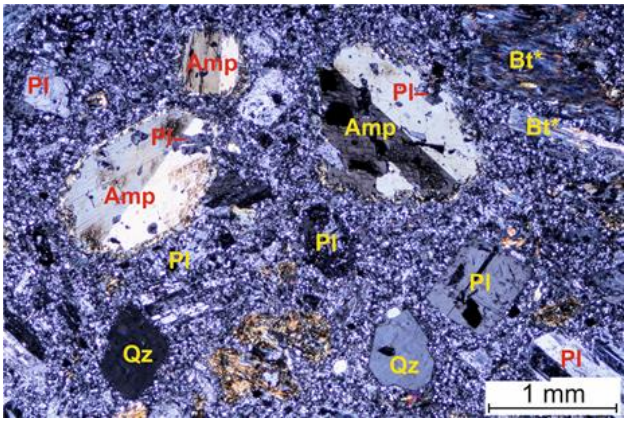


***Figure 18b.***

*Thin-section image (Fig. 18a) and microphoto (Fig. 18b, cross-polarized light) of coarse-grained quartz-diorite porphyry with quartz. Note plagioclase enclosed in amphibole phenocrysts and resorption of quartz phenocrysts. Amphibole is replaced partially by carbonate, former biotite (Bt*) is replaced by chlorite. Groundmass shows a microallotriomorphic-granular texture.*

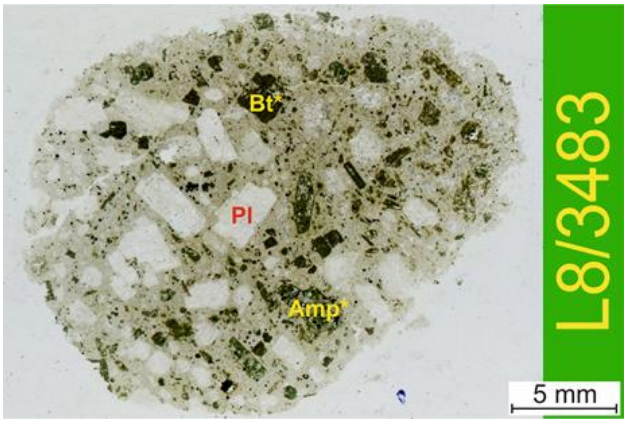


***Figure 18c.***

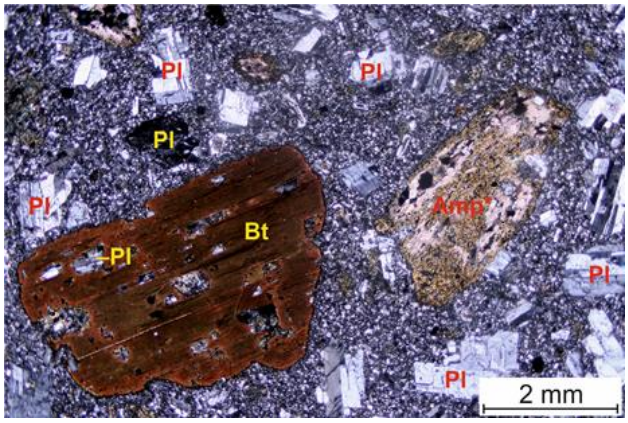


***Figure 18d.***

*Thin-section image (Fig. 18c) and microphoto (Fig. 18d, cross-polarized light) of coarse-grained quartz-diorite porphyry without quartz. Amphibole and biotite phenocrysts enclose plagioclase. Amphibole is replaced partially by carbonate, former biotite (Bt*) is replaced by chlorite. Groundmass shows a microallotriomorphic-granular texture. This type forms a sill at the locality Hodruša – tajch.*

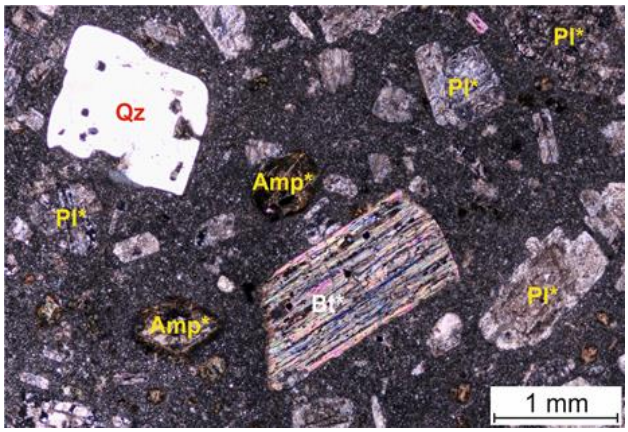


***Figure 18e.***

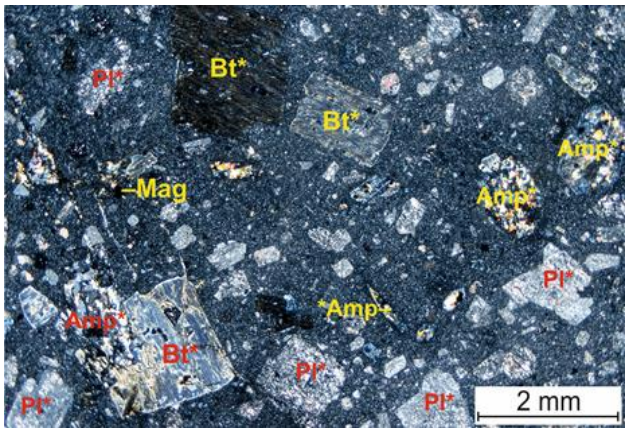


***Figure 18f.***

*Microphotos (cross-polarized light) of medium-grained quartz-diorite porphyry with quartz (Fig. 18e) and without quartz (Fig. 18f). Former plagioclase (Pl*) is replaced by carbonate and sericite, former amphibole (Amp*) is replaced by carbonate and chlorite and former biotite (Bt*) is mostly replaced by chlorite. In both types groundmass shows a fine microallotriomorphic-granular texture.*

***Figure 19a.*** *A quarry opened in a ring-dike of quartz-diorite porphyry at the locality Juraj adit. Note a pronounced blocky jointing.*

***Figure 19b.*** *A detail of the quartz-diorite porphyry at the locality Juraj adit.*

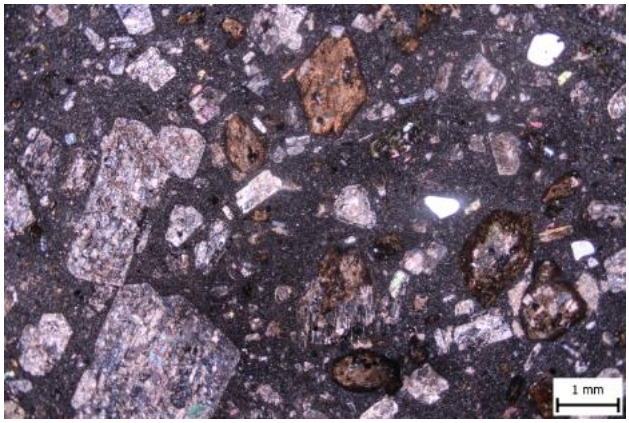


***Figure 19c.*** *Microphoto (cross polarized light) of the quartz-diorite porphyry at the locality Juraj adit. Phenocrysts of plagioclase, amphibole and biotite are altered.*

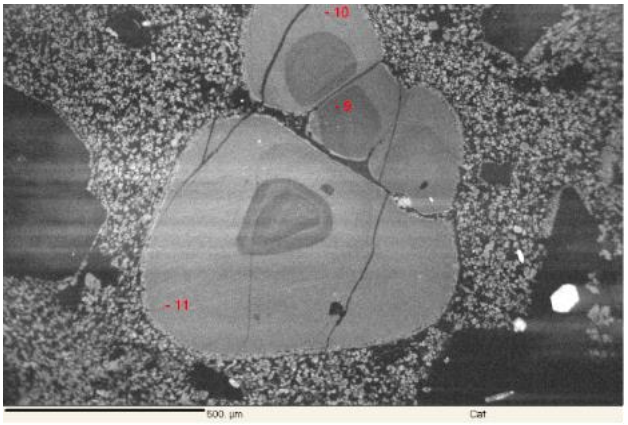


***Figure 19d.*** *CL image of quartz phenocryst in the quartz-diorite porphyry at the locality Juraj adit. Note resorbtion and zonality – darker corres are lower in Ti implying a lower temperature.*

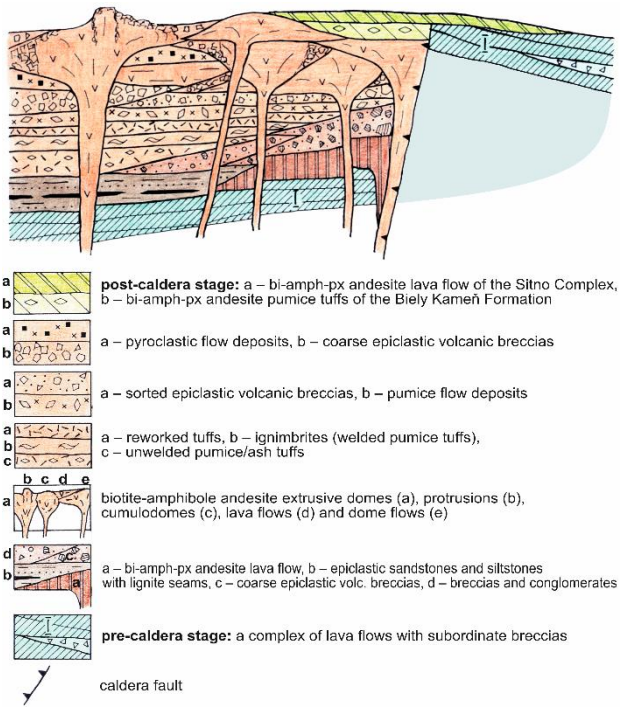


***Figure 20.*** *Scheme of the Štiavnica caldera filling. Note, that the relative thickness of volcaniclastic rocks in the lower part of the caldera filling is overestimated.*

### *3.9. Banský Studenec – the 3rd caldera stage, Studenec Formation: bt-amp andesite extrusive dome*

The Studenec Formation represents the Štiavnica Caldera filling. It extends in the thickness 200–500 m around the uplifted block of the resurgent horst and is often covered by andesite volcanic formations of the post-caldera stage along the margins of the caldera (Fig. 1). Tuffaceous sediments with rare lignite seams make up the lowermost part of the succession in the central part of the caldera, while breccias occur along the caldera margins (coarse material from the caldera walls). Dome/flow complexes of felsic biotite-amphibole andesites represent most of the filling, being accompanied by coarse extrusive breccias, block and ash pyroclastic flow deposits, pumice flow deposits, reworked tuffs and epiclastic volcanic

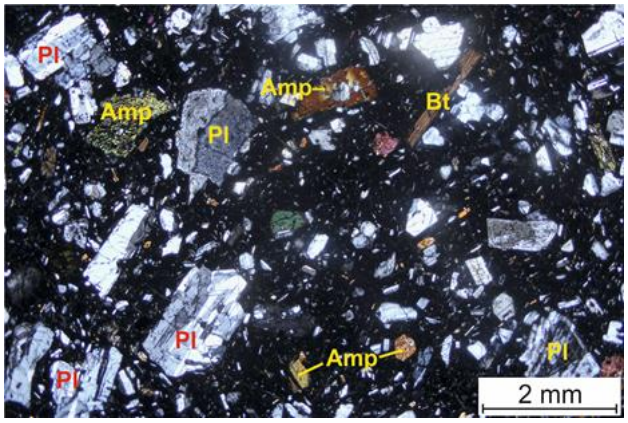


***Figure 21a.***

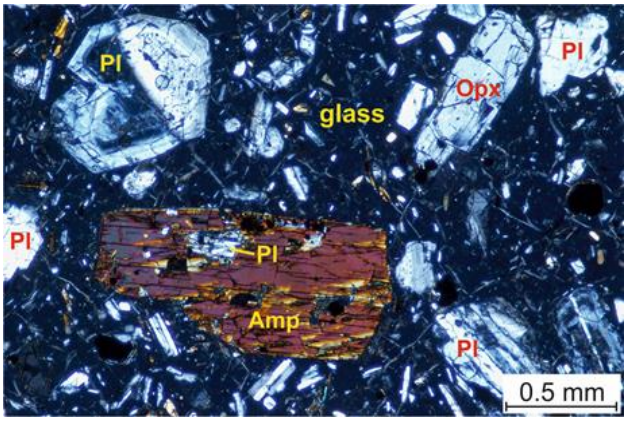


***Figure 21b.***

*Microphotos (cross-polarized light) of glassy biotite-amphibole andesite. Note a sporadic orthopyroxene phenocryst, a zonal plagioclase phenocryst with resorbed core and an idiomorphic plagioclase grain enclosed in amphibole phenocryst.*

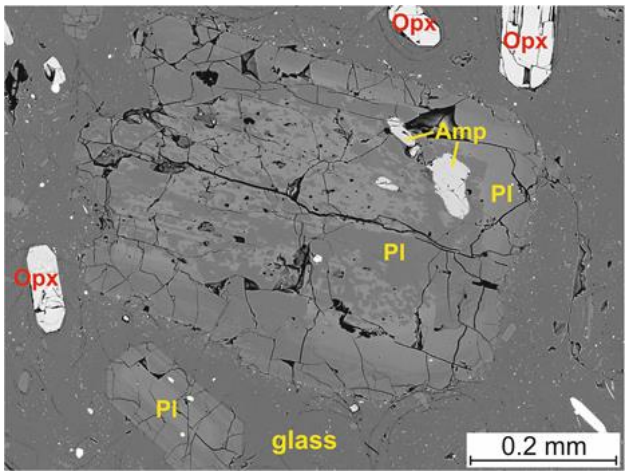


***Figure 21c.***

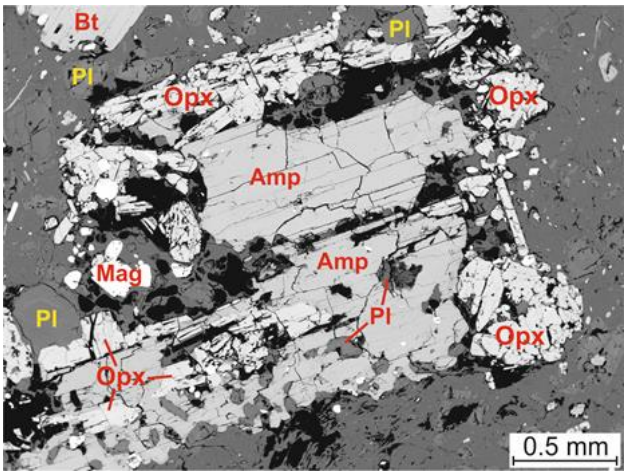


***Figure 21d.***

*BSE images of phenocrysts in glassy biotite-amphibole andesite. Plagioclase phenocryst showing a resorbed core with patchy zoning and enclosed grains of amphibole (Fig. 21c). Amphibole phenocryst with enclosed plagioclase grains showing a rection rim of orthopyroxene grains. Both images indicate mixing of evolved magma with intermediate/mafic magma (Fig. 21b).*

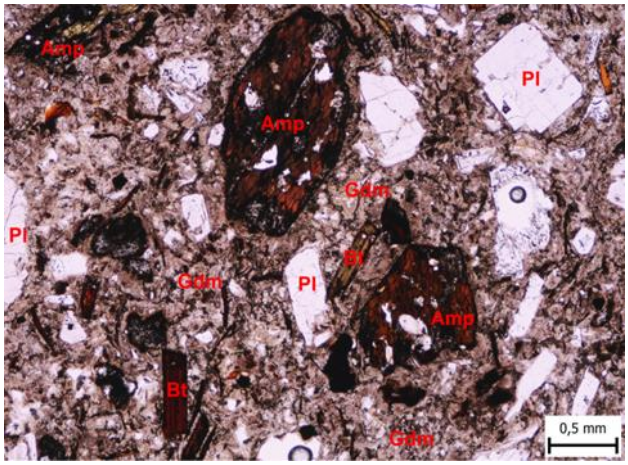


***Figure 21e.*** *Microphoto of biotite-amphibole andesite from the locality Banský Studenec. Note a partial opacitization of mafic minerals by hematite.*

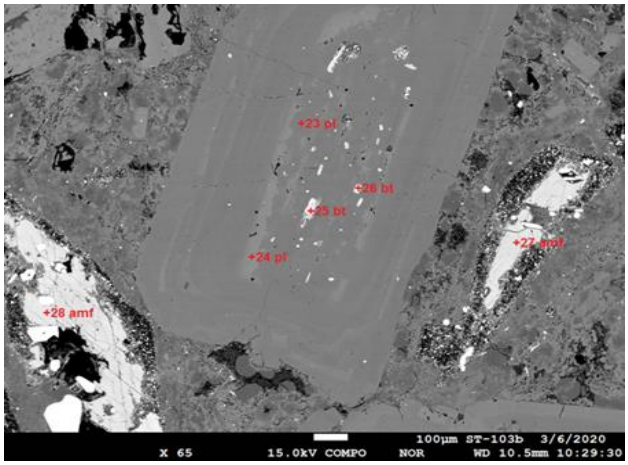


***Figure 21f.*** *A resorbed core of a plagioclase phenocryst with melt and biotite inclusions – an evidence of magma mixing.*

breccias (Fig. 20). Felsic andesite lava flows and epiclastic volcanic breccias occur also beyond margins of the caldera as fillings of radially oriented valleys on slopes of the stratovolcano.

Biotite-amphibole andesites of the caldera fill are not petrografically uniform. Phenocryst assemblages as well as groundmass textures are variable. Andesites with phenocrysts of plagioclase, amphibole, biotite and minor orthopyroxene dominate (Fig 21a). Less frequent there are those with phenocrysts of plagioclase, amphibole, biotite and those compositionally at the andesite/dacite boundary with phenocrysts of plagioclase, amphibole, biotite and minor resorbed quartz. Size of phenocrysts varies mostly in the range 0.5–4 mm, bigger ones up to 6–7 mm (especially amphiboles) are less frequent or rare. Phenocryst content is 30–40 %. Groundmass texture is variably hyaline, hyalopilitic, microlitic with glass, hyalo-spherulitic or microlitic-granular (in the case of dikes) with glass or feldspars and quartz as dominat phases.

Prismatic plagioclase phenocrysts show intergrowths with amphibole and biotite phenocrysts. Their magmatic zonality is not uniform. Mostly the uniform core is surrounded by inconspicuous oscilatory zoning concluded by the An-poor zone at the edge. A significant part of plagioclase grains shows resorbed An-poorer cores replaced by in patchy zoning and surrounded by the An-rich zone (Fig. 21c and d; along with sporadic mafic encalves evidence of magma mixing). Plagioclase grains include frequently tiny grains of magnetite, ilmenite, apatite and zircon, in the case of resorbed cores also ortopyroxene, biotite and/or amfibole, usually in association with melt inclusions (Fig. 21f). Prismatic to acicular amphibole grains are variably intergrown with and/or enclose smaller idiomorphic grains of plagioclase, orthopyroxene, biotite and/or magnetite. Biotite books are mostly thin, variably intergrown with plagioclase and amphibole. they enclose smaller idiomorphic grains of plagioclase and magnetite. Both, amphibole and biotite phenocrysts enclose magnetite, ilmenite, apatite and zircon as tiny inclusions. Quartz phenocrysts are resorbed and in cathodo-luminiscence images show inconspicuous zoning. Smaller magnetite grains enclose sometimes idiomorphic grains of plagioclase and apatite. Biotite-amphibole andesites are generally not affected by hydrothermal alterations. Oxidized porous varieties of a pink to brown color show opacitization of mafic minerals and groundmass by hematite.

At the locality Banský Studenec there is exposed an internal part of one of the biotite-amphibole andesite extrusive domes. The andesite is massive, showing an irregular blocky jointing. It is medium/coarse porphyritic with phenocrysts of plagioclase, amphibole and biotite in groundmass showing a hyalo-spherulitic/felsitic texture (Fig. 21e). A part of plagioclase phenocrysts shows resorbed cores with inclusions of biotite, amfibole and/or melt (Fig. 21f) as evidence of mixing with mafic magma.

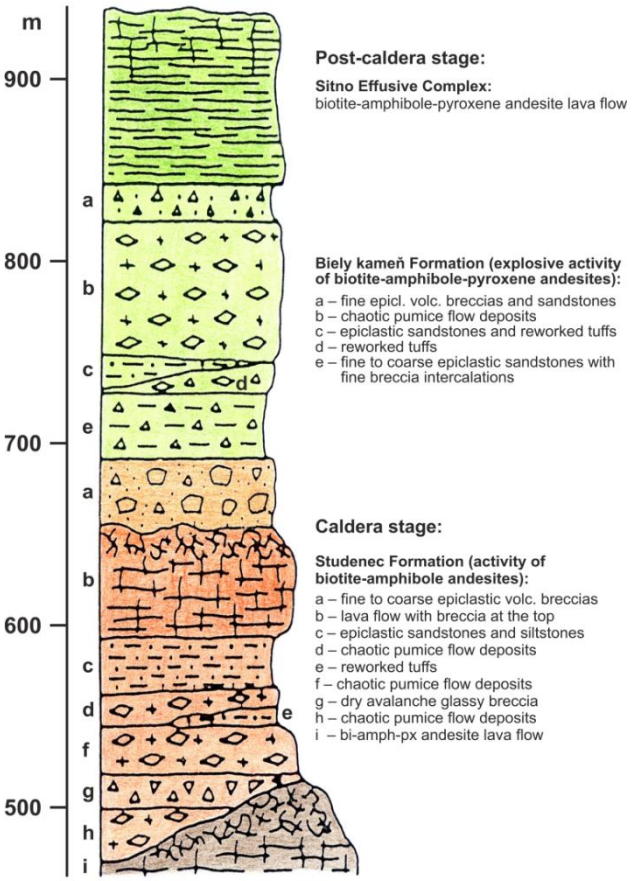


***Figure 22.*** *Lithostratigraphic column next to the village Ilija in the southern part of the Štiavnica caldera.*

### *3.10. Ilija – the 3rd caldera stage, Studenec Formation: bt-amph andesite pumice flow deposits*

For a general description of the Studenec Formation see the locality Banský Studenec above.

The visited locality is situated in the southern part of the Štiavnica caldera, next to the village Ilija, where pyroclastic rocks dominate in the lower part of its filling (Fig. 22). Following an emplacement of the early biotite-amphibole-pyroxene andesite lava flow the plinian type explosive activity created a succession of pumice flow deposits that are interbedded with a horizon of glassy dry avalanche deposit from a nearby dome and products of their reworking. Overlying epiclastic volcanic sandstones and siltstones indicate a break in volcanic activity that was followed by emplacement of a thick biotite-amphibole andesite lava flow and accumulation of coarse epiclastic volcanic breccias.

At the locality there is in an abandoned quarry exposed a thick horizon of pumice flow deposits (Fig. 23a), corresponding to the layer “d” in the Fig. 22. Chaotic, unsorted and un-welded deposits are composed of pale pumice fragments (mostly 2–3 cm, max. up to 8 cm in diameter) dispersed in unsorted tuffaceous matrix (small pumice, coarse to fine ash and crystals of plagioclase, amphibole and biotite) (Fig. 23b–d). There are present also rare fragments of older andesites. As far as

***Figure 23a.*** *Pumice flow deposits in the village Ilija are compact, showing an irregular blocky jointing.*

***Figure 23b.*** *Pumice flow deposits show a chaotic, matrix-supported texture.*

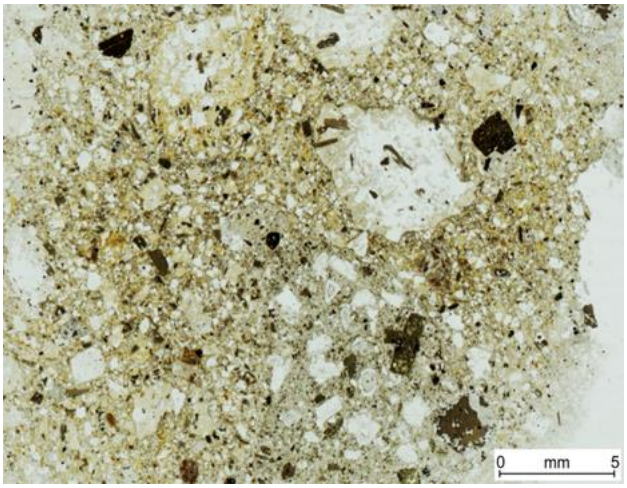


***Figure 23c.*** *A thin-section the matrix composition – small pumice fragments, ash affected by diagenetic processes and crystals of plagioclase, amphibole and biotite.*

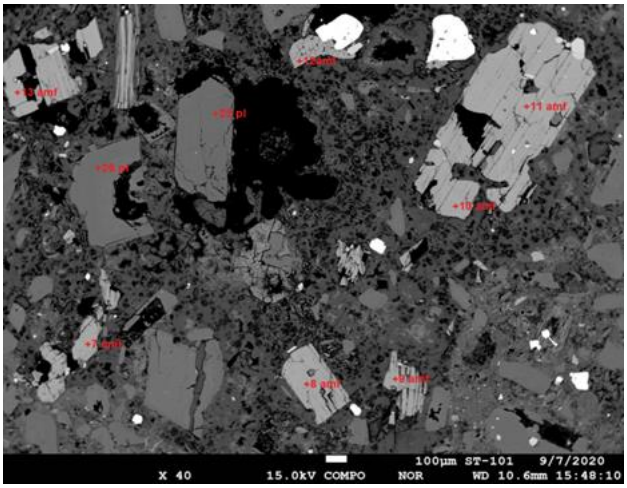


***Figure 23d.*** *BSE image documents the matrix composition.*

petrography is concerned pumice and ash represent biotite-amphibole andesite with porous glassy groundmass (Fig. 23c–d). Owing to their easy formatting and good thermal insulation pumice flow tuffs have been in the past used extensively for construction of houses in the village.

## References


Chernyshev I.V., Konečný V., Lexa J., Kovalenker V.A., Jeleň S., Lebedev V.A. & Goltsman Y.V. (2013): Geologica Carpathica, 64, 327–351.

Lexa J., Štohl J. & Konečný V. (1999): Mineralium Deposita, 34, 639–654.

Lexa J., Yi K., Broska I., Cieselska Z., Koděra P., Kohút M., Mathur R., Prcúch J., Szczerba M., Uhlík P. & Vojtko R. (2025): Geologica Carpathica, 76, 1–24.

Konečný V., Lexa J., Halouzka R., Hók J., Vozár J., Dublan L., Nagy A., Šimon L., Havrila M., Ivanička J., Hojstričová V., Mihaliková A., Vozárová A., Konečný P., Kováčiková M., Filo M., Marcin D., Klukanová A., Liščák P. & Žáková E. (1998a): Explanations to the geological map of the Štiavnické vrchy and Pohronský Inovec Mountains (Štiavnica Stratovolcano). Geological Survey of Slovak Republic, Bratislava.

Konečný V., Lexa J., Halouzka R., Dublan L., Šimon L., Stolár M., Nagy A., Polák M., Vozár J., Havrila M., Pristaš J., (1998b): Geological map of the Štiavnické vrchy and Pohronský Inovec Mountains (Štiavnica Stratovolcano) 1:50 000. The Geological Survey of Slovak Republic, Bratislava.

Kubač A., Chovan M., Koděra P., Kyle J.R., Žitňan P., Lexa J. & Vojtko R. (2018): Mineralogy and Petrology, 112, 705–731.

Kumar S. (1995): Geologica Carpathica, 46, 379–382.

Rottier B., Audetat A., Koděra P. & Lexa J. (2020): Volcanology and Geothermal Research, 401, 106967

Tomek F., Žák J. & Chadima, M. (2014) Bulletin of Volcanology, 76, 873.

# METALLOGENY OF THE BANSKÁ ŠTIAVNICA REGION

Peter Koděra[1] & Jaroslav Lexa[2]
[1] Comenius University, Department of Mineralogy, Petrology and Economic Geology, Bratislava, Slovakia
[2] Earth Science Institute, Slovak Academy of Sciences, Bratislava, Slovakia

## 1. Itinerary

**Leader: Peter KODĚRA**

8:00: Departure from Nagybörzsöny

9:00 - 12:30: Morning excursion

Banská Štiavnica – Kalvária hill – spectacular view of the Banská Štiavnica town and overview of local geology

Banská Hodruša - All Saints Historical Adit and Mineralogical Museum – introduction to mineral deposits of Štiavnica stratovolcano, medieval underground works on Ag-Au epithermal veins, mineral collections

12:30 - 13:00: Lunch (lunch-packs)

13:00 - 18:00: Afternoon excursion

Banská Hodruša – ore heaps of the active Rozália mine, Au-Ag-Pb-Zn-Cu ore from epithermal veins

Banská Štiavnica – Glanzenberg – medieval open pit mine excavations on the Au-Ag-Pb-Zn-Cu Špitaler Ag-Au-Pb-Zn epithermal vein

18:00: Guided tour in Banská Štiavnica and Gala Dinner

## 2. Introduction to geology and metallogeny of the Štiavnica stratovolcano

The Štiavnica Stratovolcano is the most extensive and complex volcanic edifice among the Miocene to Quaternary volcanoes of the Carpathian-Pannonian region that hosts the world-class Banská Štiavnica - Hodruša ore district. It has well-preserved volcanic formations and complexes in the proximal and distal zones (Fig. 1) that allowed for a serious paleovolcanic reconstruction (Konečný et al., 1998; Chernyshev et al., 2013). The most characteristic features of the volcano include an extensive caldera, a late-stage resurgent horst in the caldera centre and a large subvolcanic intrusive complex. Magmas associated with the hydrothermal mineralization were sourced from an upper crustal reservoir (1 to 3 kbar at 960 to 700 °C) that was active more than 3 million years (Rottier et al., 2020). Ore deposits formed during periods of reservoir cooling when the residual melt reached fluid saturation. A resurgent horst in the central part of its caldera exposes subvolcanic intrusive complexes and related ore mineralizations (Fig. 2).

The edifice of the Štiavnica Stratovolcano represents a succession of volcanic formations and complexes with a common central zone and outward dipping volcanic slopes that corresponds to the protracted evolution of a transcrustal magmatic system (Rottier et al., 2020). Its structure and evolution in five essential stages, originally compiled by Konečný et al. (1998a,b) have been recently treated by Chernyshev et al. (2013) and Lexa et al. (2025). Evolution of the stratovolcano is summarized in Fig. 3.

During the **1st stage** (15.0–13.6 Ma, **pre-caldera stage**) volcanic activity of px and amph-px andesites, interrupted by periods of quiescence and related erosion, created a succession of stratovolcanic complexes and formations. Paleovolcanic reconstruction points to remnants of a large stratovolcanic edifice, 40 km in diameter at the base of a compound volcanic cone, surrounded by accumulations of epiclastic volcanic rocks. In the central zone of the edifice, rocks of the pre-caldera stage are exposed in the eastern half of the resurgent horst. Here, the former stratovolcanic edifice has been deeply eroded and is built mostly of andesite sills and laccoliths emplaced in the lower part of the edifice. The pre-caldera stage also comprises a stock of bt-amph-px diorite porphyry south of the caldera (~14.5 Ma, **stage 1b**) that hosts a sub-economic Beluj Au-porphyry mineralization.

During the **2nd stage** in the evolution of the Štiavnica Stratovolcano edifice (13.6–12.9 Ma) a break in volcanic activity, extensive denudation in its central zone, and emplacement of subvolcanic/intravolcanic intrusions took place. The subvolcanic/intravolcanic intrusive complex is exposed in the uplifted block of the resurgent horst in the central zone of the volcano. The oldest diorite intrusion (~14.8 Ma) is the parental intrusion of the barren Šobov high-sulfidation hydrothermal system. A younger granodiorite bell-jar pluton (~13.44 Ma, **stage 2a**), emplaced by the underground cauldron subsidence mechanism, invaded basement rocks especially using subhorizontal discontinuities in the Mesozoic sedimentary formations above the Variscan crystalline rocks. Three types of mineralizations are associated with the emplacement of the granodiorite bell-jar pluton. At contacts of the pluton with basement carbonate rocks there are magnetite skarn deposits and occurrences. In

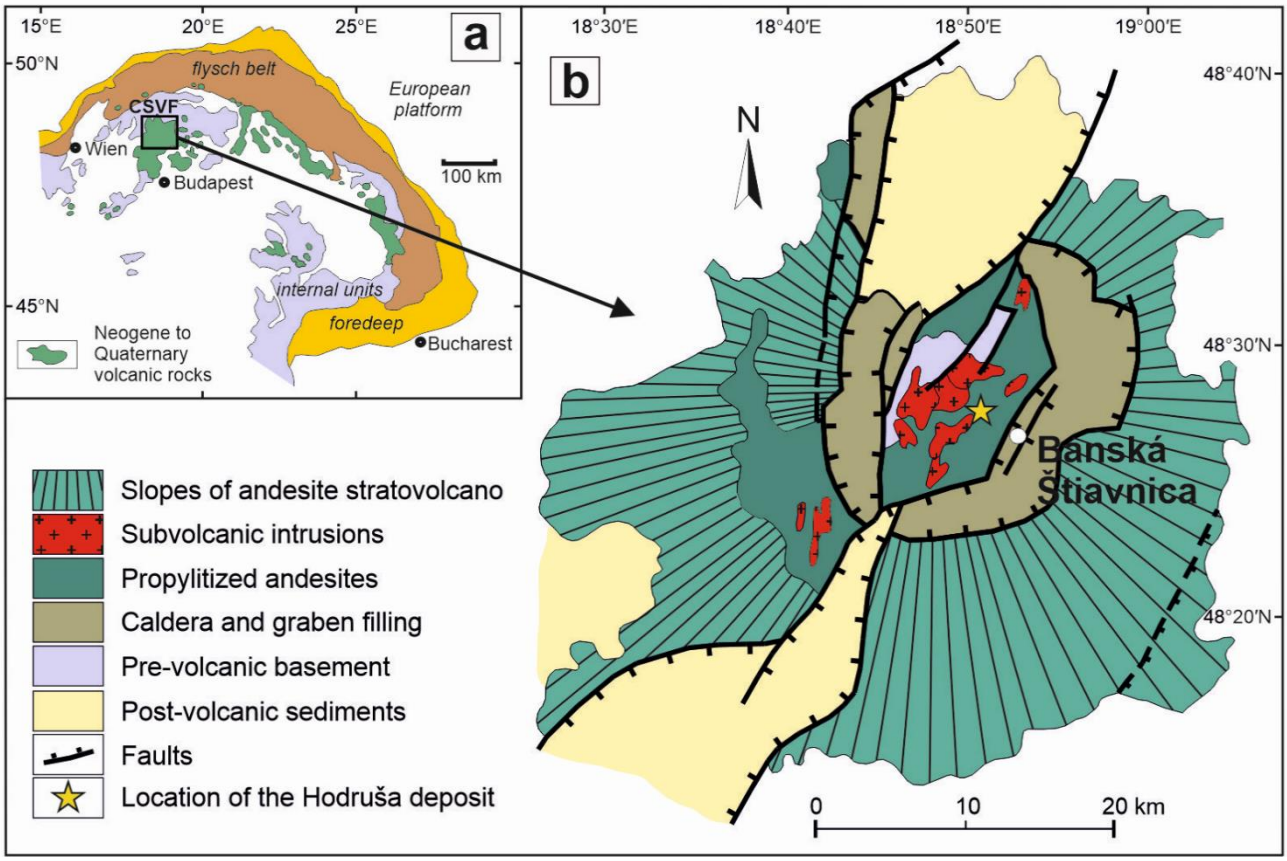


***Figure 1.*** *Regional setting of the study area: (a) Position of the Central Slovakia Volcanic Field within the Neogene to Quarternary volcanics of the Carpathian arc and Pannonian basin. (b) Structural scheme of the Štiavnica stratovolcano.*

the central part of the pluton the overlying pre-caldera stage andesites are affected by extensive advanced argillic alteration, while underlying granodiorite and fragments of basement rocks host a stockwork-disseminated base metal mineralization. Kubač et al. (2018) revealed that the extensive denudation was related to a resurgent uplift of the granodiorite pluton and associated sector collapse at the SE side of the edifice in the interval 13.44–13.3 Ma. A basal, low angle detachment/ shear zone hosts the Hodruša precious/base metal epithermal mineralization.

Quartz-diorite porphyry sills (**stage 2b**) invaded major subhorizontal discontinuities in the basement, granodiorite pluton, contact of basement and volcanic complex and overlying andesites of the pre-caldera stage. Sills emplaced among andesites occur especially in the area of the sector collapse where they intrude structures of the shear zone, both low angle faults as well as moderately dipping tension faults (Kubač et al., 2018). Emplacement of sills (13.3–13.0 Ma) post-dated the precious/base metal mineralization of the shear zone, except for few thin sills parallel with the roof of the granodiorite that were emplaced before the mineralization and the granodiorite pluton emplacement (~13.60 Ma). Further eastward the sills pass into moderately outward dipping ring dikes.

Granodiorite to quartz-diorite porphyry dike clusters and small stocks (~12.9 Ma, **stage 2c**) are situated at the periphery of the granodiorite pluton (Figs. 2 and 3). Stocks with roof pendants in basement rocks pass upward into dike clusters emplaced in andesites of the pre-caldera stage. Intrusions of granodiorite porphyry are accompanied by the Cu-Au skarn-porphyry type mineralization. Quartz-diorite porphyry dikes extend in the western and northern parts of the resurgent horst, outside of the sills extent. They are mostly thin, either vertical or dipping inward, showing some aspects of cone sheets. They post-date granodiorite porphyry stocks/dike clusters and quartz-diorite porphyry sills.

During the **3rd stage** (~12.9 Ma, **caldera stage**) subsidence of the Štiavnica caldera took place. Related volcanic activity filled the caldera and formed contemporaneous volcanic deposits on slopes of the Štiavnica Stratovolcano edifice. The caldera is 20 km in diameter (Fig. 1) and the extent of its subsidence is estimated at 500 m. It is not of an explosive type, but it is filled by bt-amph andesite/dacite extrusive domes, dome flows and associated pyroclastic and epiclastic volcanic rocks. Tuffaceous sediments at the base of the caldera filling and underlying andesites of the pre-caldera stage are locally affected by advanced argillic alteration showing typical features of hot-spring type systems. Andesites of the caldera fill at its eastern part host a barren Varta high-sulfidation hydrothermal system with advanced argillic alteration.

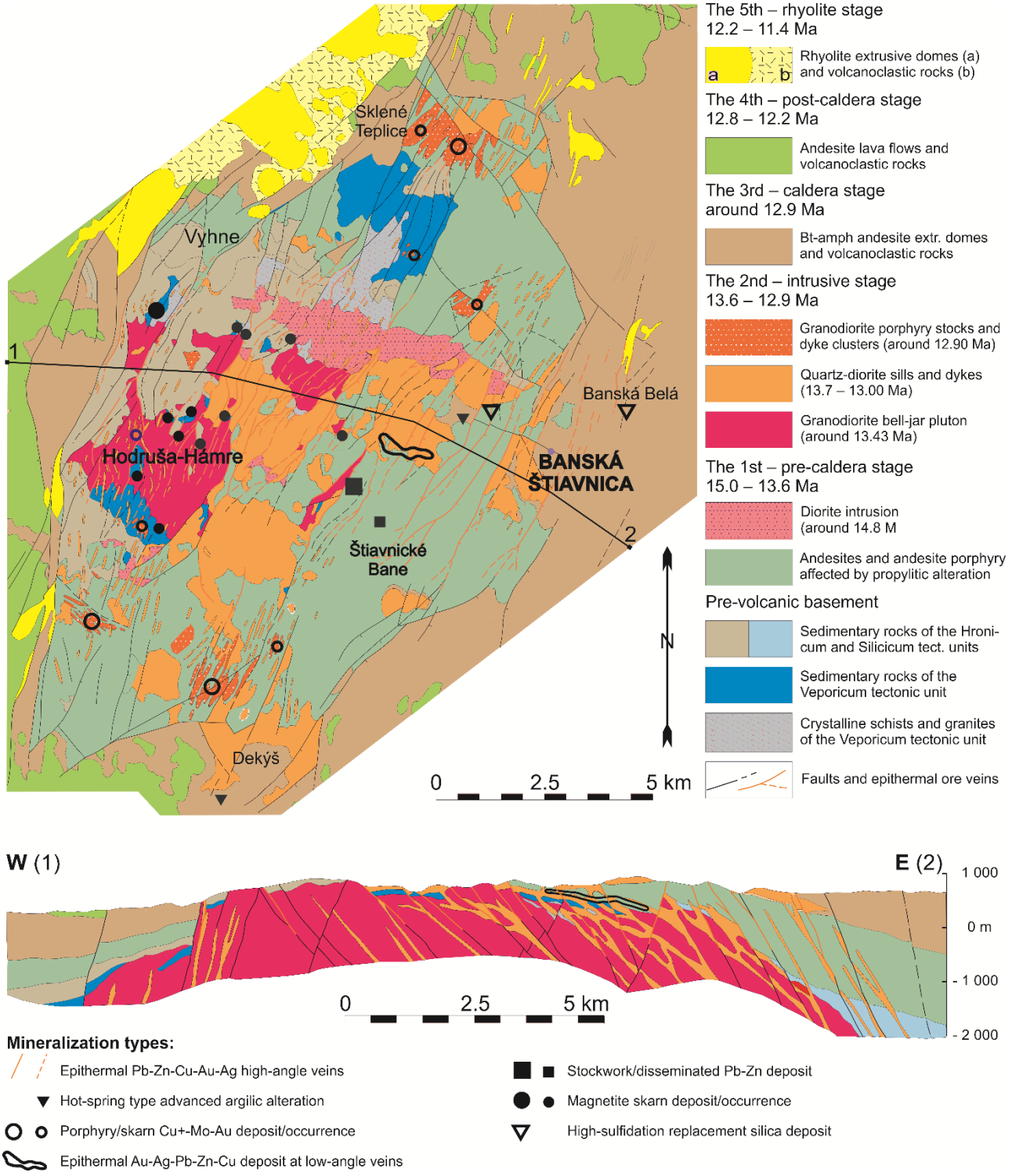


***Figure 2.*** *Structural scheme and section of the resurgent horst in the center of the Štiavnica Stratovolcano caldera with the location of main mineralization types. Modified after Lexa et al. (1999).*

During the **4th stage** (12.8–12.3 Ma, **post-caldera stage**) a renewed activity of less evolved andesites created explosive, stratovolcanic and effusive volcanic complexes/formations that rest upon caldera fill and outside of the caldera on slopes of the Štiavnica Stratovolcano edifice. Individual complexes/formations are spatially limited to certain sectors of the edifice. In the distal zone they pass into aprons of epiclastic volcanic breccias, conglomerates and sandstones.

During the **5th stage** (12.3–11.4 Ma) rhyolite volcanic activity created dikes, cryptodomes and extrusive domes on N S to NE-SW striking faults, including marginal faults of a contemporaneous resurgent horst in the central part of the caldera and local horsts west of the caldera. An

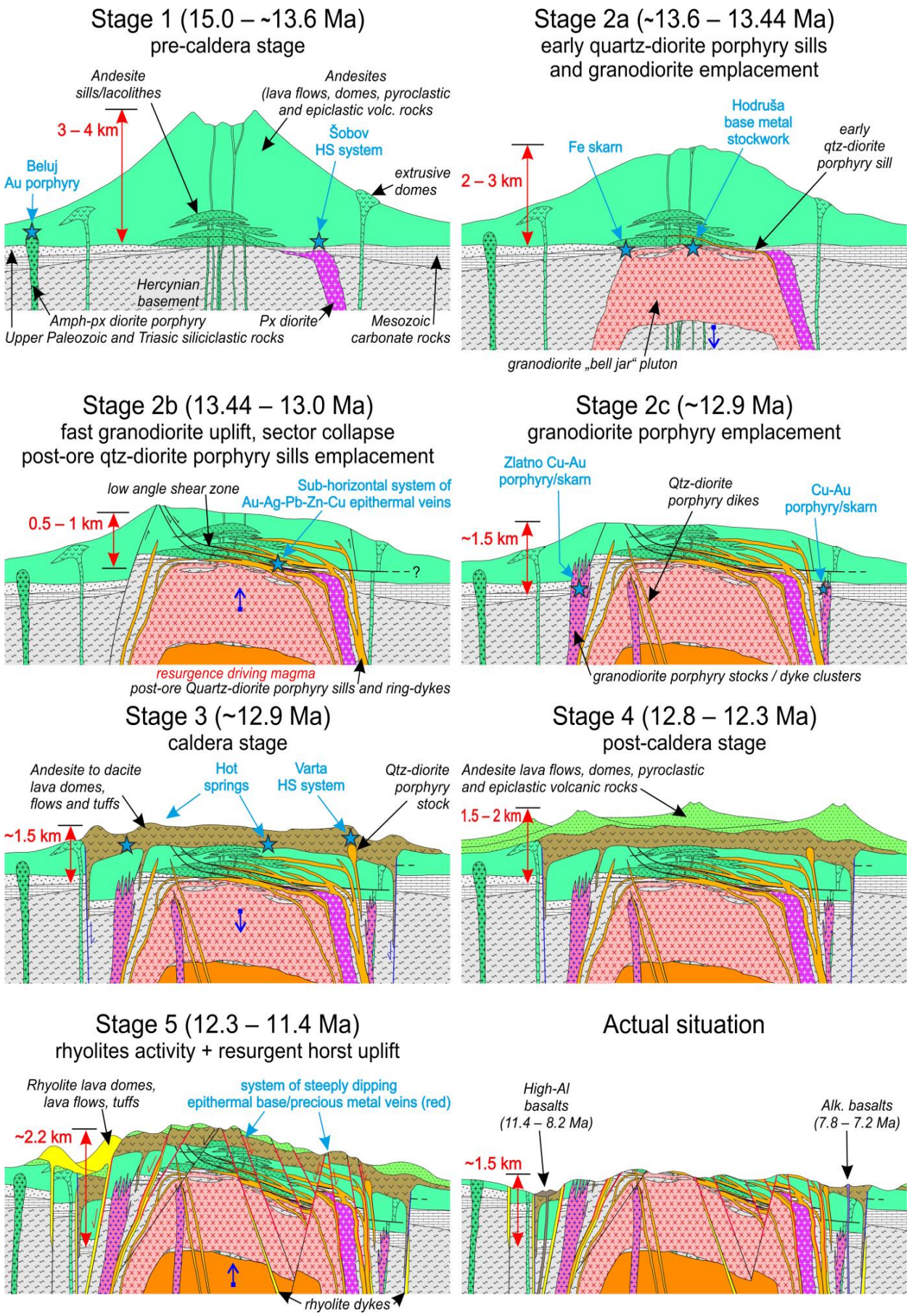


***Figure 3.*** *Evolution of the Štiavnica Stratovolcano edifice and associated mineralizations (Lexa et al. 2025).*

extensive dome/flow complex with related pyroclastic and epiclastic rocks spreads along southeastern and eastern marginal faults of the Žiar depression in the northern sector of the Štiavnica Stratovolcano edifice. Faults of the resurgent horsts host also an extensive system of intermediate to low-sulfidation precious/base metal epithermal veins. The hydrothermal system and rhyolite activity were contemporaneous.

Štiavnica stratovolcano is one of the largest ore districts in the Carpathian arc, famous for its long-lived silver and gold mining of epithermal veins. Central zone of the volcano contains four distinct vein systems, briefly characterised in Tab. 1 and Fig. 4. The earliest vein system (13.44–13.31 Ma) consists of precious and base metal veins of intermediate sulfidation type, currently mined at the Rozália mine in Hodruša, while the extensiver later system of low to intermediate sulfidation types correspond to hydrothermal activity during the long-lasting uplift of the resurgent horst in the centre of the caldera (12.2–10.9 Ma).

## 3. History of mining in the Štiavnica stratovolcano (after Bakos et al., 2004)

The Hodruša-Štiavnica ore district occurs in two major ore fields. Banská Štiavnica ore field is located in the vicinity of the Banská Štiavnica town and host predominantly the sulphide-rich "Štiavnica type" veins. Hodruša ore field occurs in the vicinity of the Hodruša village and hosts predominantly the silver-rich "Hodruša type" veins. Based on archive data, the estimated total historical output of mines in the entire Štiavnica-Hodruša district is some 4,000 t of Ag and 80 t of Au. Base-metal mining, which was active from the 19$^{th}$ century until 1992, resulted in some 70,000 t Zn, 55,000 t Pb and 8,000 t Cu (Lexa et al., 1999).

Banská Štiavnica is believed to be the oldest mining town of Slovakia. The town used to be rightly given the nickname "mother of medieval mining towns", as it has belonged to the most important mining towns of historical Hungary and leading European centres of technical progress and culture. The town has played prominent role in worldwide development of mining, dressing and smelting.

Celtic prospectors colonised the area between 3$^{rd}$ and 2$^{nd}$ century BC, and commenced with gold panning. The first record on ore exploitation comes from 969 AD. In these times, the Slavic inhabitants have given the most important settlement beneath Paradajz hill the name Štiavnica. The name of settlement was respected and took over by Saxonian colonists, who came here in the second half of 12$^{th}$ century and transcribed the original name as Schemnitz.

Banská Štiavnica obtained municipal and mining rights still in the times of the king Bela IV (1235–1270). Favourable development of Banská Štiavnica was interrupted in 1442 as a consequence of long-lasting struggle for Hungarian throne. Moreover, the town was stricken with a strong earthquake in the next year. Mining has been in blossom in the second half of 15$^{th}$ century, however, progress of mining has been hampered by the need of pumping mine waters, what forced the miners to join into greater companies.

Exploitation of the Banská Štiavnica ore field have gradually transferred from the oxidation zone to deeper, less enriched primary ores. On 8$^{th}$ of February 1627, Gaspar Weindl of Tyrol realized the world-first blast with help of gunpowder in the Horná Bieber adit. In the 17$^{th}$ century, the waters have been pumped out towards levels of heritage adits with kits, leather bags and piston pumps. Man´s power and draught animals have driven the pumping facilities. A total of 5,040–5,600 kg of silver has been recovered annually in the years 1600–1625, and 2,800–3,360 kg in the period between 1626 and 1650. 14,933.52 kg of silver and 187.04 kg of gold has been obtained annually between 1672 and 1680. The year 1690, with recovery of 29,000 kg of silver and 605 kg of gold, was the most successful year in the whole history of the Banská Štiavnica ore field.

The 18th century brought recession in the recovery of precious metals. Only exceptionally the exploitation was maintained at higher levels. The annual yield in the period between 1740 and 1823 has been only 145 kg of gold and 8,900 kg of silver in average. New technological inventions in the ore dressing have demanded construction of additional water dams. In the period between 1500 and 1638, only four dams have existed in the surroundings of Banská Štiavnica, but their number increased to 14 in the second half of the 18$^{th}$ century. The Hell´s pumping machine based on hydraulic principle and powered by water was a unique device introduced in 1755 in the Amália shaft. Successive completion of three prominent heritage adits has been of great importance for the efficient drainage of mine waters. Sluices have been widely used for ore processing in the 18$^{th}$ century. Vanners have been introduced in Banská Štiavnica for the first time in Europe. Gold concentrates have been amalgamated with mercury, burned and delivered to coinage factories. In 1789, Ignac Born improved the gold and silver dressing by introducing the indirect amalgamation with chloride roasting.

The state mines of Banská Štiavnica faced the first deficit in the second half of the 18$^{th}$ century and authorities for the first time seriously speculated about the termination of mining works. In the years 1946 and 1947, still 16,400 tonnes of ores grading 3.1 g/t of Au and 17 g/t of Ag was recovered, but the exploitation of precious metals definitely ceased in 1947 and was substituted with that of base metals that lasted until 1992.

In the Hodruša ore field mining of precious metals has been known from the 13$^{th}$ century, but the Hodruša settlement have existed since 1352. The exploitation in Hodruša was in blossom in 16$^{th}$ century, when mining companies were created. As many as 136 such companies existed in 1616 exploiting the veins in upper part of the

***Table 1.*** *Basic characteristics of epithermal vein mineralization in the central zone of the Štiavnica stratovolcano. Ages of volcanic rocks and mineralisation are from Chernyshev et al. (2013) and Lexa et al. (2025).*

| Deposit or vein system | Rozália mine (Banská Hodruša) | Banská Štiavnica | Hodruša | Banská Belá, Kopanice, Vyhne |
|---|---|---|---|---|
| **Location** | W central part - underground only | E, SE and central part of the horst | Central, W, NW parts of the horst | Marginal parts of the horst (E, W, S) |
| **Main metals** | Au-Ag-Pb-Zn-Cu | Pb-Zn-Cu ± Au-Ag | Ag ± Au-Pb-Zn | Au-Ag ± Pb-Zn-Cu |
| **Genetically related volcanics, their age** | Qtz-diorite porphyry 13.6–13.0 Ma | | Rhyolite 12.3–11.4 Ma | |
| **Age of mineralisation** | 13.44–13.31 Ma | | 12.2–10.9 Ma | |
| **Sulfidation state** | Intermediate | Intermediate | Intermediate to low | Low |
| **Major ore minerals** | Gold, El, Sph, Ga, Ccp, Ag-Au tellurides | Ga, Sph, Ccp, Py ± Ag sulfosalts, El | Prg-Prs, Pol-Prc, Ste ± El, Ga, Sph, Ccp, Py | Ag-sulfosalts, El ± Ccp, Ga, Sph, Py/Mc |
| **Major gangue minerals** | Qtz, Mn-Car, Rhd | Qtz, Mn-Car, Rhd | Car, Qtz | Qtz, Car |
| **Ag-Au ratio of ores** | 1:1 to 10:1 | 10:1 to 20:1 | 100:1 | 1:1 to 10:1 |
| **Alteration** | Illite, Ad, Qtz | Illite, Qtz, Ad | Illite, I/S, Ad, Qtz | Qtz, Ad, I, I-S |
| **Fluids properties** (salinity in NaCl eq.) | < 3 wt% 280-330 °C boiling | < 11 wt% <100-380 °C, mixing, boiling | < 6 wt% 200-300 °C boiling | < 3 wt% 220-260 °C boiling |
| **Main references** | Maťo et al., 1996, Koděra et al., 2005; Kubač et al., 2018 | Koděra, 1963; Kovalenker et al., 1991, 2006 | Označila et al., 1993; Majzlan, 2009, Majzlan et al., 2016 | Lexa et al., 1997; Berkh et al., 2014 |

**Mineral abbreviations:** El = electrum, Sph = sphalerite, Ga = galena, Ccp = chalcopyrite, Py = pyrite, Mc = marcasite, Pol = polybasite, Prc = pearceite, Prg = pyrargyrite, Prs = proustite, Ste = stephanite, Qtz = quartz, Car = carbonate, Rhd = rodonite, I-S = illite-smectite, Ad = adularia

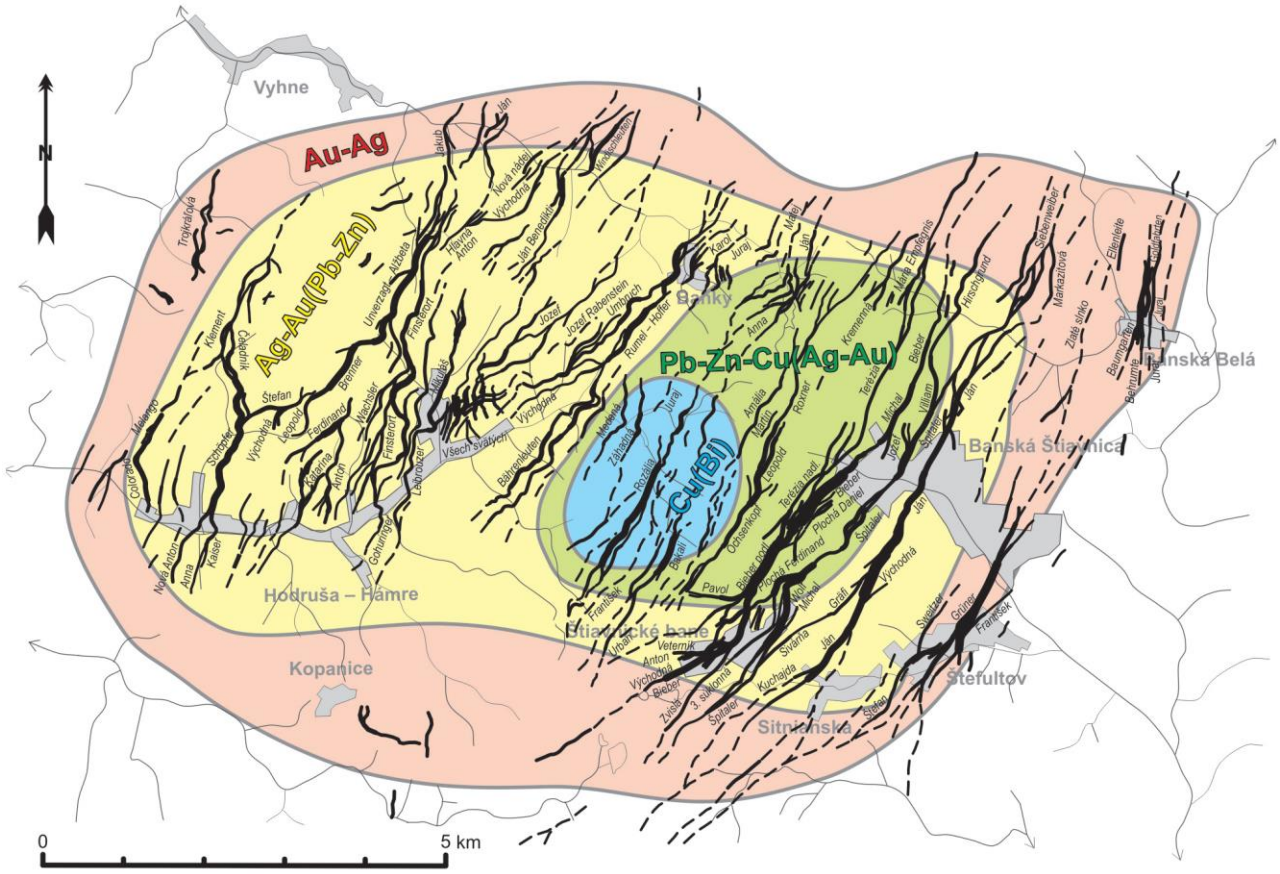


***Figure 4.*** *System of post-caldera epithermal veins in the central zone of the Štiavnica stratovolcano with predominant metals zoning (after Smolka & Lexa, 2002).*

village, other veins started to be mined in the second half of the 18th and in the 19th century. Recovery and dressing the gold-silver ores terminated in 1950 due to depletion of reserves. Since 1951, all mining activities in Hodruša have been concentrated on the recovery and dressing the copper ores from the Rozália mine, where it has continued up to 1991 (Rozália vein is on the westernmost Štiavnica-type sulphide-rich veins).

Owing to lack of water as the main source of energy, a sophisticated system of water dams, drains and races has been created. Water has been utilised for pumping mine waters, driving the traction shaft machines, stamps, and for ore jigging. Still in second half of the 19th century, a total of 25 dressing factories have worked in the whole Hodruša valley. Since 1929, the stamp dressing has been replaced by flotation.

Mine waters have caused serious problems during exploitation of deeper parts of the veins. The Hodruša Heritage Adit, obtained an approval of a heritage adit already in 1494 and was draining out all significant mines in Hodruša. It was completed in 1765 and with the length of 12,149 km, it has been the longest mining work in the World in these times. The Voznica Heritage Adit called also the Heritage Adit of the Emperor Joseph 16.5 km long has been constructed in the period between 1782 and 1878. The adit has extended from the Hron river beneath the Hodruša valley and massif of the Tanád Hill to Banská Štiavnica and has drained all significant veins of the entire ore district. In the time of completion, it was again the longest mining work in the World. The New Drainage Adit has been driven between 1975 and 1994, in total length of 13.8 km, with the intention to replace the Voznica Heritage Adit but was never put in action due to termination of mining in Banská Štiavnica.

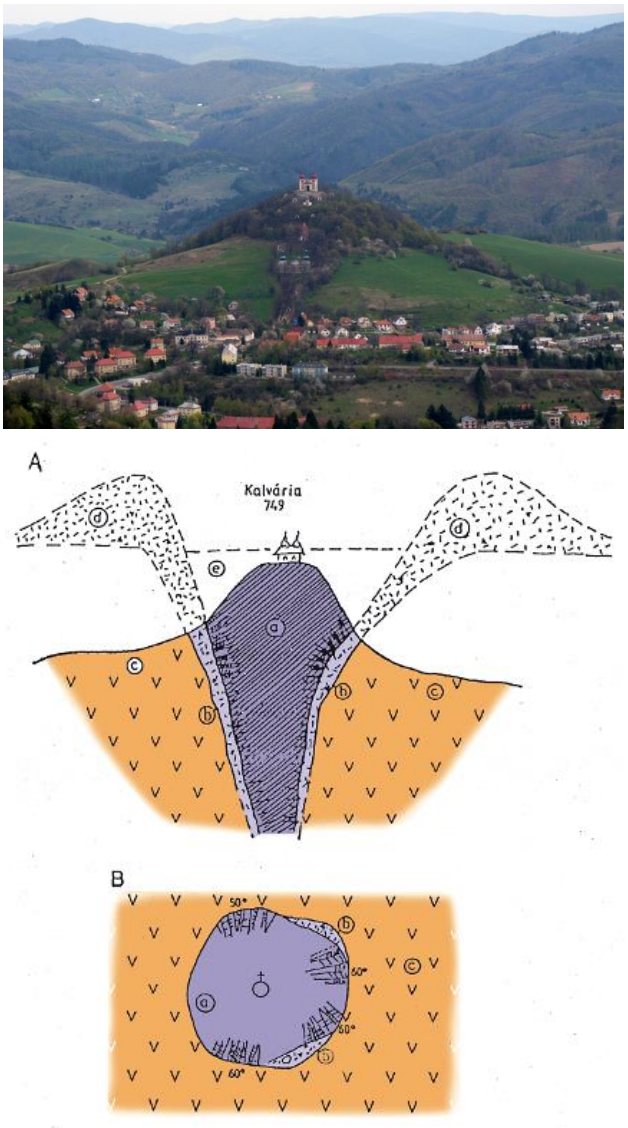


***Figure 5.*** *Alkali basalt neck forms a prominent hill that hosts a baroque church and stations of the cross. Section (A) and floor plan (B) of the Kalvária neck: a – basalt showing columnar jointing; b – diatreme breccia; c – bt-amp andesite; d – assumed former maar eliminated by erosion; assumed lava lake filling the maar. Photo and drawing by Konečný* [2].

## 4. Field stops

### *4.1. Banská Štiavnica – Kalvária Hill*

The alkali basalt neck Kalvária next to the city of Banská Štiavnica represents one of five alkali basalt occurrences in the Central Slovakia Volcanic Field. With the age around 7.3 Ma (Kantor & Wiegerová, 1981; Konečný et al., 1999) it is the oldest one, while Putikov vŕšok volcano next to Nová Baňa with the age around 130 Ka (Šimon & Halouzka, 1996) is the youngest one. The neck represents remnants of a maar-diatreme volcano created by phreatomagmatic explosive activity (Fig. 5). The early stage of diatreme and maar formation is preserved only as remnants of tuffaceous breccia (diatreme filling) at the edges of the neck. Tuff ring of the maar was completely denudated by subsequent erosion. The late stage of basalt lava inflow created a lava lake filling the former maar crater. Outward dipping columns along the edges of the neck confirm such interpretation. The present form of the neck is a result of surrounding rocks denudation that did not affected massive basalt of the neck.

From the petrographic point of view alkali basalt of the neck is nepheline basanite with phenocrysts of olivine and clinopyroxene in microcrystalline groundmass composed of plagioclase, olivine, clinopyroxene, nepheline, analcime, leucite? and opaque minerals.

This stop provides a spectacular view of the central zone of the Štiavnica stratovolcano and the Banská Štiavnica town.

[2] https://apl.geology.sk/g_vgl/content.jsp?cislo=VK-10&jazyk=EN

### *4.2. All Saints Historical Adit (mining museum)*

The mining museum in Hodruša makes access to old mining works on the All Saints vein and related hanging wall stockwork, which belongs to a system of epithermal veins evolved on and controlled by faults of the resurgent horst uplifted in the central part of the caldera. The uplift lasted almost 2 mil. years (~12.5–10.7 Ma, Lexa et al., 1999). Associated hydrothermal activity formed an extensive epithermal system including 120 veins and veinlets, covering almost 100 km2 (Lexa et al., 1999; Fig. 4). Regional stress field during this time was dominated by a strong NW-SE extension, with the maximum stress axis mostly in the subvertical position (Nemčok et al., 2000). Veins are associated with the emplacement of rhyolite extrusive domes and dykes that took place especially along marginal faults in the most uplifted W and NW parts of the horst. Long-lasting evolution of the hydrothermal system related to the structural evolution of the horst resulted in a considerable variability of epithermal veins. Their general zoning can be described in terms of four concentric zones: the most temperate Cu zone in the centre is surrounded successively by the base metal, silver-gold and the outside gold-silver zones (Fig. 4). On the basis of structural aspects, vertical extent, spatial distribution and dominant mineral paragenesis three types epithermal veins can be recognized (Lexa et al., 1999): sulphide rich base metal veins ± Au in the east/central part of the horst ("Štiavnica type"), Ag-Au ± base metal veins in the central/western part of the horst ("Hodruša type" – includes All Saints vein), Au-Ag veins related to marginal faults of the horst ("Kremnica type").

The central Ag-rich and sulphide-rich veins are probably the oldest veins, while the marginal Au-Ag veins are the youngest. Vein systems show a large variability in mineral content with numerous stages and substages and Au:Ag ratios (1:1 to 1:100). Fluid properties have generally changed from more saline (>10 wt% NaCl eq.) and rather hot (>300°C) towards less saline (<3 wt% NaCl eq.) and moderate temperate (<260°C) with evidence for boiling and mixing. The zonal arrangement of vein systems probably results from continuous, long-lasting uplift of the horst with subsequent transfer of hydrothermal activity from the centre to the margins of the horst. Very different vertical extent of the individual vein systems (central sulphide-rich <1000 m, Ag-rich 200–500 m, marginal Au-Ag < 300 m) with only a sparse presence of base metals in deepest parts of the Ag-rich and Au-rich vein systems indicate, that differences in erosion level of the vein systems had only a minor influence on the zonal arrangement of veins observed today (Kovalenker et al., 1991; Lexa et al., 1997; Berkh et al., 2014; Majzlan et al., 2016).

Silver-rich Ag-Au ± base metal veins in surroundings of Hodruša ("Hodruša type") evolved on N-S to NE-SW striking faults in the central, western and northwestern parts of the resurgent horst. The length of individual veins does not exceed 3 km, but many of the veins are much shorter. Veins dipping 30–50° E or SE dominate, the extent of displacement being in the range 40–200 m (Fig. 6). Some of the veins split close to the surface into a number of veinlets and branches, including antithetic ones, creating stockwork-like structures accompanied by extensive alterations. This feature indicates much smaller erosion of veins in comparison with the Štiavnica type veins. Vertical extent of individual veins varies in the range 200-500 m, so their original vertical extent probably did not exceed 800 m. Koděra (1965, 1989) has defined 9 mineralization stages, dominated by quartz or carbonates and minor base metal sulphides. Upper parts of veins are enriched in silver minerals and electrum, while deeper parts are relatively enriched in base metal sulphides. Surficial parts of the veins, which were the object of the initial, very successful medieval mining, were considerably enriched by oxidation and cementation processes (up to 60 g/t Au and 3 000 g/t Ag). Alteration zones of the veins are more extensive compared to the Štiavnica-type veins, especially in the case of stockwork-like vein structures (Onačila et al., 1993).

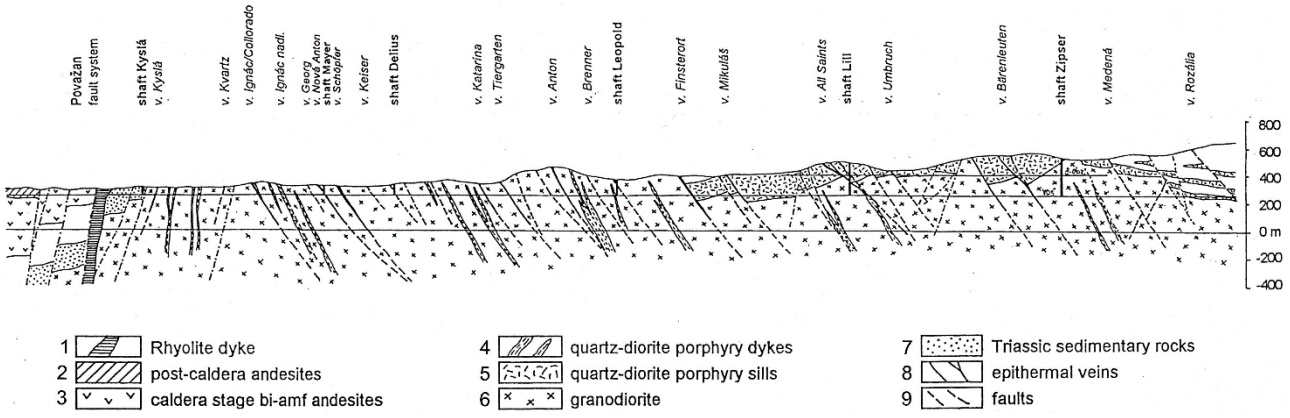


***Figure 6.*** *Transverse sections of the system of silver ± base metal epithermal veins along the Hodruša and Voznica historic adits in the Hodruša ore field (Lexa et al., 1997).*

The All Saints vein was one of the most important ones among the Hodruša type silver ± base metal epithermal veins (Lexa, 1999). Its exploitation took place mostly during the 16th century. The NE-SW striking vein dipping 25–35° southeast represents one of the en-echelon arranged veins among the Nicholas vein at the west and Rummel-Hoffer vein at the east as the master faults (Onačila et al., 1993). Footwall and hanging wall of the vein is represented by granodiorite and quartz-diorite porphyry (Fig. 7). The vein is about 1,200 m long and 2–3 m thick. It was exploited down to the level +224 m, making accessible the vertical extent of 400 m. Hanging wall includes several vein branches and numerous small veinlets, including the antithetic ones, creating a weakly mineralized stockwork. The stockwork enabled intense silicification and adularization of hanging wall rocks giving rise to metasomatic quartzites and adularia enriched rocks.

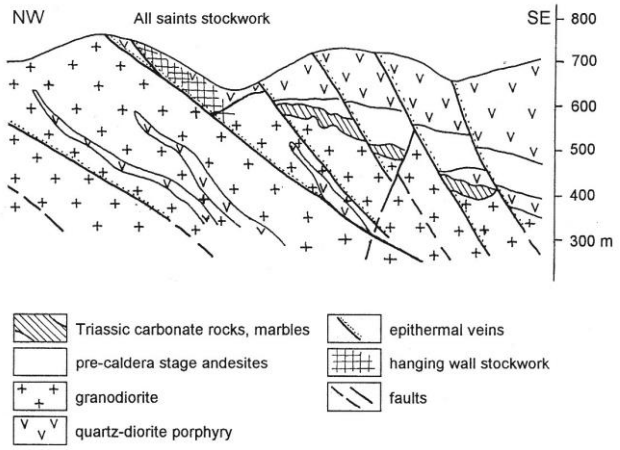


***Figure 7.*** *Section along the All Saints vein and stockwork in Hodruša (Onačila et al., 1993).*

The vein is formed by quartz or quartz-carbonate gangue with sulphides and silver sulphosalts, which are concentrated in the lower and upper parts of the vein around the central mass of quartz (Onačila et al., 1993). Mineable ore continued sometimes also into the hanging wall branches and stockwork. Electrum of the fineness 470–600 is present in the form of minute grains (5–200 micrometers) in base metal sulphides, along their boundaries and along boundaries of quartz and carbonate grains. Electrum as well as younger silver sulphosalts also replace the older base metal sulphides. Grade of the ore at the lowermost horizon was 0.62 % Pb, 1.21 % Zn, 0.26 % Cu, 0.52 g/t Au and 36.1 g/t Ag (Smolka et al., 1993).

### *4.3. Banská Hodruša –ore heaps of the active Rozália mine*

The Au-Ag-Pb-Zn-Cu epithermal deposit Banská Hodruša of intermediate-sulphidation type is the last active ore mine in Slovakia, with estimated total production ~10 t Au and 6 t Ag (Kubač et al., 2018). This deposit occurs at the historical Rozália mine 400 – 650 m below the current surface and it represents an unusual subhorizontal multi-stage vein system, hosted by a shear zone, corresponding to a low-angle normal fault zone (LANF).

Epithermal Au-rich ore has been exploited in the Rozália mine since 1993, but in the past this mine was also used to exploit steep Cu-Pb-Zn epithermal veins and a base-metal stockwork mineralization. Au-rich veins were unexpectedly discovered during drilling program on northern continuation of the Bakali vein (Cu-Pb-Zn Štiavnica type vein) in 1988. It was a new style of Au mineralization atypical for the district as a whole. After confirmation of drilling results mining exploration started from the 14th level of the historic Rozália mine, at that time accessible only 100 m from the discovery point. The exploitation at this mine is still in progress but the peak annual production of nearly 500 kg of gold was reached between the years 1994 and 1997. A complex genetic model of the mineralisation was published by Koděra et al. (2023) and is summarised below.

Mineralisations at the Rozália mine: The Au-Ag-Pb-Zn-Cu epithermal veins, hosted by the shear zone, occur in the pre-caldera andesites near the flat roof of a granodiorite pluton (Fig. 8). The ore deposit developed in several stages (Kubač et al., 2018). The early stage consists of low-grade silicified breccia at the base of the deposit, occurring along E-W oriented subhorizontal structures dipping 20-30° to SE. The main ore mineralisation consists of stockwork of early steep veins (E-W, 40-60° to S) and a later system of veins inside the shear zone (NE-SW, ~45° to SE), accompanied by complementary detachment-hosted veins (<30°) in the roof of the shear zone. Veins consist of early quartz-rhodonite assemblage (incl. Mn-carbonates, chlorite) and later sulphide-gold assemblage (incl. sphalerite, galena, chalcopyrite, pyrite, rare Te-minerals and various gangue minerals, Fig. 9). Mined ore contains 14 g/t Au, 17 g/t Ag, 0.6% Zn, 0.45% Pb, and 0.15% Cu in average. The shear zone was intruded by mostly post-mineralisation system of quartz-diorite porphyry sills. Post-ore veins include rare barren quartz veins of variable orientation mostly hosted by the porphyry. Major veins are accompanied by adularia, quartz and illite. Strong argillisation (illite ± quartz, pyrite) occurs in the roof of the shear zone (Koděra et al., 2017).

The stockwork mineralisation occurs some 1.5 km south of the Au-Ag deposit, mostly hosted by apical porphyritic part of the granodiorite pluton. It resembles a porphyry hydrothermal system including potassic alteration in the granodiorite, and advanced argillic

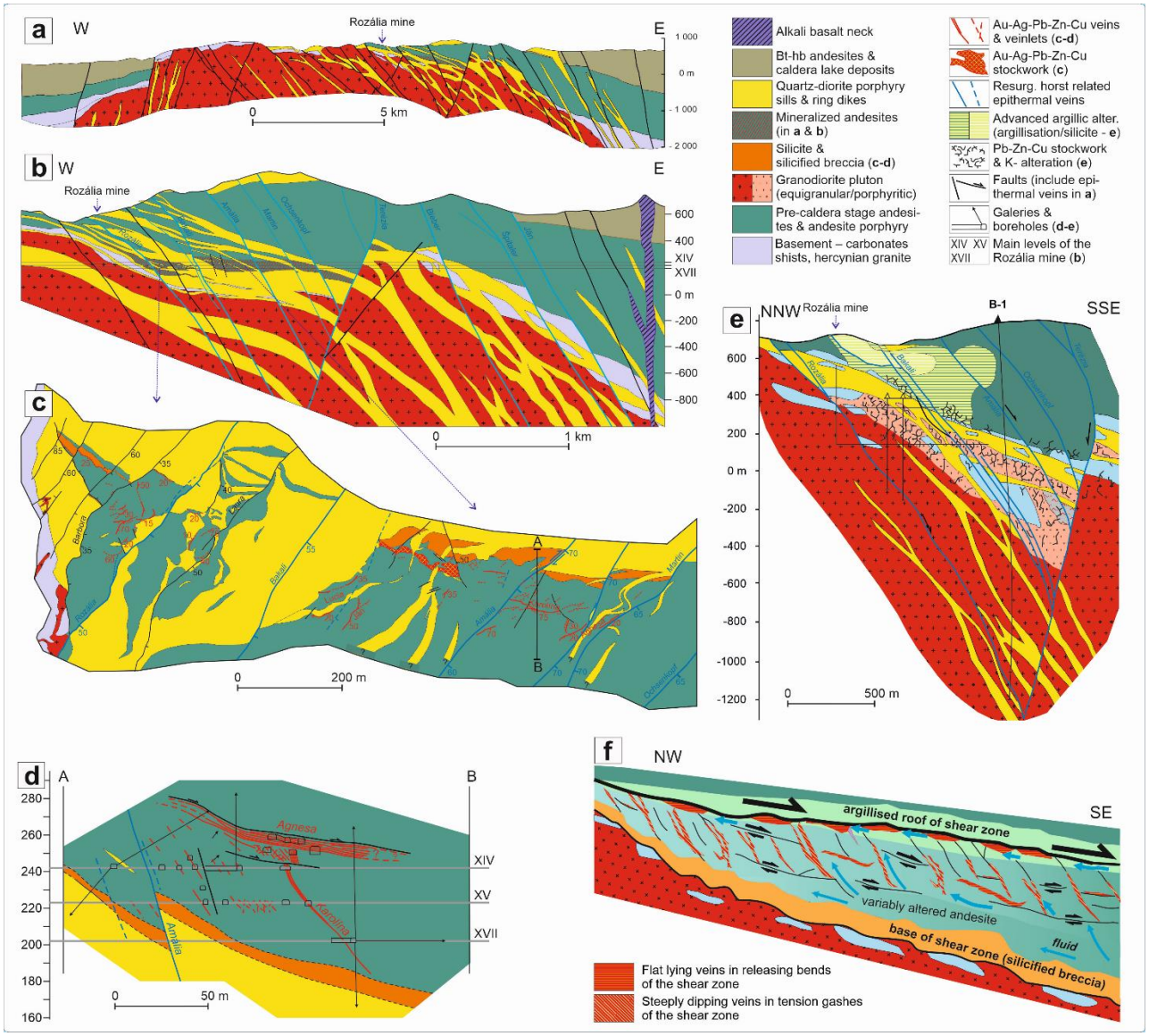


***Figure 8.*** *Geological and structural setting of the epithermal Au-Ag-Pb-Zn-Cu deposit and other mineralisations at the Rozália mine. (a) Position of the mine in the resurgent horst in the centre of the Štiavnica stratovolcano caldera. (b) A general section of the vicinity of the mine showing the position of Au-rich mineralisation. (c) Structural map of the Au-rich deposit at the 14th level of the mine. (d) Section of the deposit showing spatial relationship of major vein types. (e) Cross section through the Pb-Zn stockwork mineralization and related alteration along the B-1 drill hole and underground works of the Rozália mine. (f) Structural, fluid flow and alteration scheme of the shear zone with Au-rich veins. It consists of low-grade silicified breccia at the base of the deposit, system of steep veins inside the shear zone, accompanied by complementary detachment-hosted veins in the roof of the shear zone. Early development of the shear zone (Stage IVa) is not shown for clarity. Most ores are in areas rich in dilatational structures, where roof and top of the shear zone are relatively close together (after Kubač et al., 2018 and Koděra et al., 2004).*

alteration in overlying pre-caldera andesite (Koděra et al., 2004). Mined ores contained 2.5% Pb, 3.5% Zn, 0.4% Cu, 10 g/t Ag. Ore grades and intensity of potassium alteration decrease with depth.

The steep epithermal veins (50–70° to NE–SW) cut the base-metal stockwork, the gold-rich veins as well as quartz-diorite porphyry sills. They belong to an extensive system of veins in the central zone of the volcano with a zonal arrangement (Pb-Zn-Cu, Ag-Au, Au-Ag) and multi-stage filling (Kovalenker et al., 1991). At the Rozália mine the most important is the Rozália vein, mined for Cu-rich base metal ore (0.5–0.8% Cu, 0.2% Pb, 0.3% Zn, 10–20 g/t Ag, 0.1–0.2 g/t Au).

**Geological evolution:** Stages of evolution related to mineralisation at the Rozália mine (Tab. 2, Fig. 10) are interpreted based on the structural and magmatic evolution of the Štiavnica stratovolcano (Chernyshev et al., 2013, Rottier et al., 2019) and dating of subvolcanic intrusions and caldera filling (Lexa et al., 2025).

The first evolutionary stage (**Stage 1**) associated with mineralisations at the Rozália mine is related to the emplacement of the granodiorite magma between the prevolcanic basement and the pre-caldera andesite at a minimum depth of ~2 km (13.6 Ma). The intrusion has a relatively flat roof, probably as a consequence of a descent of the central block of basement rocks into the

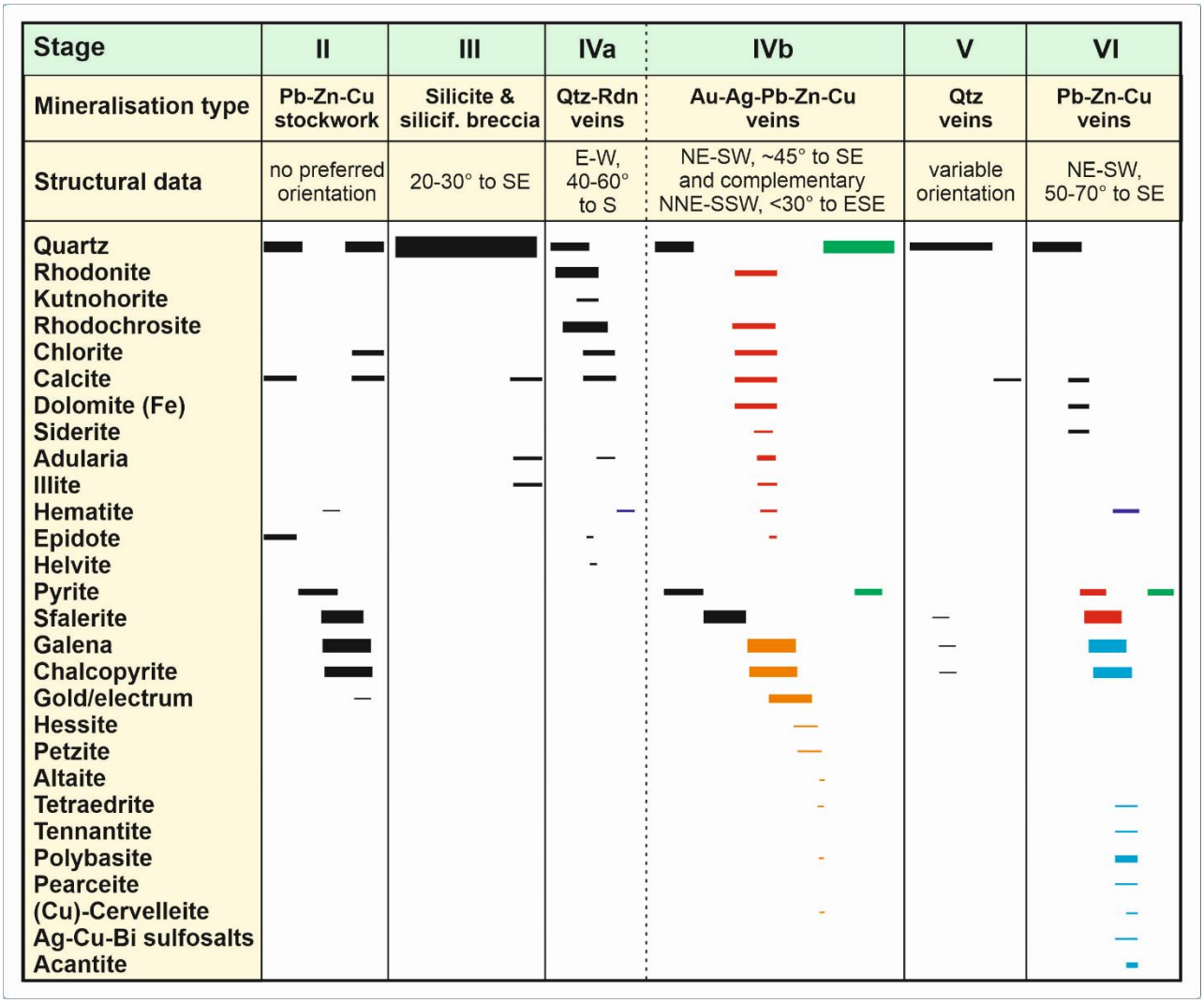


***Figure 9.*** *Paragenetic chart of epithermal mineralisation at the Rozália mine with structural data (after Kubač et al., 2018). Stages correspond to evolutionary stages presented in Fig. 10.*

upper crustal magmatic reservoir, compensated by the displacement of magma above the block. On cooling and progress of crystallization, exsolution of fluid appeared, which was responsible for adjacent Fe-skarn mineralisation and advanced argillic alteration in the apical part of the pluton (Koděra et al., 2014).

During the next four evolutionary stages, cooling and possibly mixing of the magma in the reservoir, evidenced by thermobarometry and petrography, led to its saturation by fluids and their exsolution. This caused a decrease in magma density and its migration and emplacement between the subsiding basement block and the granodiorite intrusion. Magma decompression in turn accelerated the fluid exsolution. These fluids migrated upwards using contraction cracks forming the base metal stockwork hydrothermal system (**Stage 2**) and later they penetrated the andesite-granodiorite contact forming barren silicites (**Stage 3**). The continuous emplacement of the fluid-saturated magma was also responsible for a rapid resurgent uplift and exhumation of the granodiorite pluton, finally leading to a sector collapse of the volcano, at the base with argillites, fluids-filled structures, and basement carbonates (**Stage 4**). Fluid penetration along a flat shear zone at the base of the collapse was responsible for the currently mined Au-rich veins. The accumulation of differentiated magma of lower density in the magmatic reservoir finally led to the emplacement of the post-mineralisation system of sill and dykes of quartz-diorite porphyry (13.5–13.0 Ma), especially using structures of the shear zone, and terminated the gold-forming hydrothermal activity in the area of the Rozália mine (**Stage 5**) Subsequent geological evolution of the volcano did not directly affect mineralisation at the mine. It was represented by a caldera subsidence linked with extrusive activity of evolved andesites and post-caldera andesitic effusive activity. However, fluid saturation was not reached, as magma was relatively hot (up to 970 °C), probably due to large inputs of mafic magma into the upper-crustal reservoir.

The last evolutionary stage at the mine (**Stage 6**) is related to the final cooling of the magma chamber (<750 °C), when a cupola of fluid-saturated rhyolite magma developed in the chamber, representing interstitial melt segregated from the crystal mush. Low

***Table 2.*** *Summary of geological, tectonic and fluid evolution related to all major types of mineralisation in the Rozália mine in Banská Hodruša (Koděra et al., 2023).*

| Stage | I | | II | III | IV | | V | VI |
|---|---|---|---|---|---|---|---|---|
| **Age** | **13.6 Ma** | | **13.6–13.5 Ma** | | | | **13.5–13.0 Ma** | **12.2–11.4 Ma** |
| **Mineralisation / host rock** | Fe-skarns / basement carbonates | Advanced argillic alteration / andesite | Pb-Zn-Cu stockwork / apical part of granodiorite& andesite | Silicite / subhorizont. structures in andesite in contact with granodiorite | Shear-zone hosted epithermal Au-Ag-Pb-Zn-Cu veins / andesite | | Post-mine-ralisation Qtz veins / andesite & Qtz-diorite porphyry | Pb-Zn-Cu-Ag-Au horst veins / andesite & Qtz-diorite porphyry |
| | | | | | Qtz-Rdn vein filling | Sulf-Au vein filling | | |
| **Geological evolution** | Emplacement of granodiorite pluton between prevolcanic basement and andesite, cooling, fluid exsolution during its crystallization | | Fluid saturation in magma chamber, migration of fluid-saturated magma between subsiding basement and granodiorite pluton together with continuous granodiorite uplift and exhumation | | | | | Final magma chamber cooling, cupola of fluid-saturated rhyolitic magma, horst uplift, fluid penetration into deep horst faults |
| | | | Penetration of fluids into contraction cracks | Penetration of fluid into andesite-granodiorite contact | Sectoral collapse of volcano at the base with argillites, fluids-filled structures, and basement carbonates; fluid penetration in the shear zone | | Emplacement of most sill of Qtz-diorite porphyry | |
| **Tectonic evolution** | Contraction cracking of granodiorite during cooling in subsolidus conditions | | Fracturing due to relict contraction-nal stress & hydraulic fracturing | Subhorizon. structures above the granodiorite& hydraulic fracturing | Initial N-S movement on shear zone | NW-SE reorientation of movement on shear zone | Ring and subhorizontal structures at sides and above granodiorite | Resurgent horst uplift in caldera centre, system of steep faults |
| **Fluid evolution** | Heterogenisation of fluids exsolved from granodiorite magma | | Continued fluid exsolution from magma chamber, ascend in the form of supercritical fluids | | | | | Ascend of supercritical fluids |
| | Brine cooling & mixing with meteoric water | Vapor conden-santion | Mixing of magmatic - meteoric fluids | Cooling of magmatic fluids | Boiling of magmatic fluid due to decompression | | No data | Boiling and mixing of magmatic - meteoric fluids |

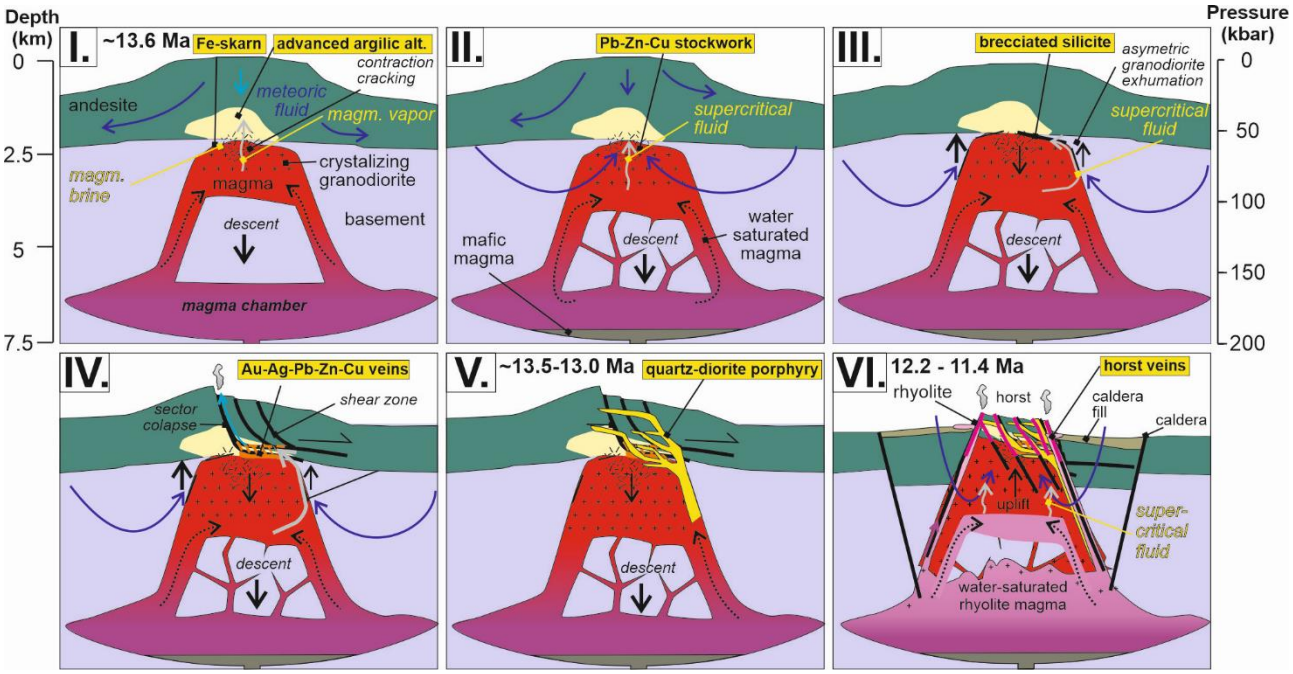


***Figure 10.*** *Stages and timing of geological evolution related to various mineralisation types at the Rozália mine, including corresponding tectonic and fluid evolution (Koděra et al., 2023).*

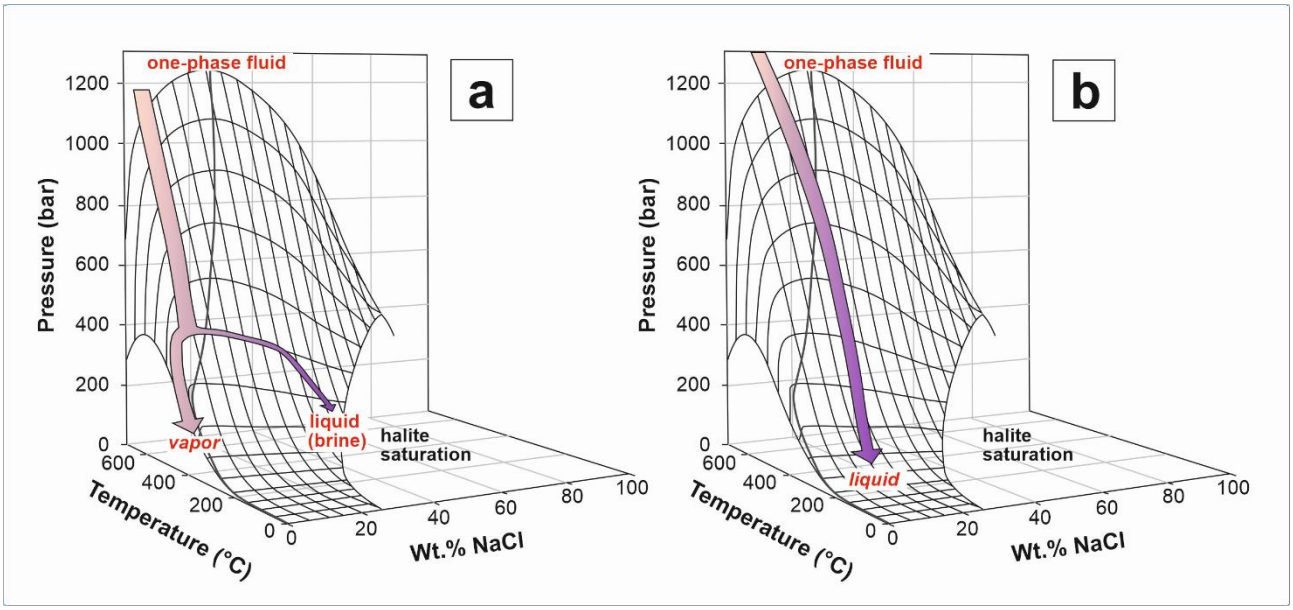


***Figure 11.*** *Idealised fluid evolution paths related to mineralisations at the Rozália mine and in its vicinity. (a) Stage I mineralisations are associated with fluid heterogenisation due to pressure drop of magmatic fluids ascending from the crystalising granodiorite pluton. (b) Stage II to VI mineralisations are associated with magmatic fluids exsolved from an upper-crustal magma chamber, while cooling under high pressure prevented fluid heterogenisation and the fluid contracted directly to liquid. After Heinrich (2007).*

density of the fluid saturated magma resulted in an uplift of the central zone of the volcano, forming a resurgent horst dome, and emplacement of rhyolite dikes and domes (12.2–11.4 Ma, outside the mine). Penetration of exsolved fluid into deep horst faults resulted in an extensive system of horst-related epithermal veins.

**Tectonic evolution:** Tectonic events and development of fractures were important for creation of fluid flow paths and the origin of various mineralisations at the Rozália mine. Tectonic evolution related to mineralisation is based on regional-scale and mine-scale structural analyses (Nemčok et al., 2000; Kubač et al., 2018).

The early base metal stockwork is related to a relict contractional stress in the granodiorite during cooling of the apical part of the intrusion, further enhanced by hydraulic fracturing. The resulting network of fractures enabled migration of fluids exsolving from the magma reservoir.

Silicites and silicified breccias of hydraulic fracturing on subhorizontal structures at the andesite-granodiorite contact are linked to the subsidence of the basement block into the upper-crustal magma chamber, including the solidified granodiorite pluton. Magmatic fluids released from the chamber penetrated the contact at a pressure close lithostatic.

Epithermal Au-Ag-Pb-Zn-Cu veins are related to the origin of the shear zone during the sector collapse of the volcano and the shear zone creation. The early movement on the shear zone was N–S oriented, forming an early stockwork of E–W oriented veins. Later movements on the shear zone were NW–SE oriented, forming a later system of veins of NE–SW orientation. Post-ore emplacement of quartz-diorite porphyry magma was enabled by the same subhorizontal structures as the ore veins and fed from ring structures, both related to the reactivated underground cauldron subsidence of the central block.

Latest base metal epithermal veins are hosted by a complex system of steep NE–SW oriented faults related to the long-lasting resurgent horst uplift.

**Fluid evolution:** Evolution of fluids related to the various stages of mineralisation at the mine is interpreted from stable isotope, fluid inclusion and illite thermometry data from the skarn and base metal stockwork mineralisation (Koděra et al., 2004), from the gold-rich veins (Koděra et al., 2005; Kubač et al., 2018) and from the horst-related base metal veins (Kovalenker et al., 1991, Koděra et al., 2005), including recent LA-ICP-MS of fluid inclusions (Koděra et al., 2019, 2021).

Inclusions in quartz from the granodiorite showed that the magmatic fluid exsolved from the granodiorite magma experienced a phase separation into a hot (>600°C) hypersaline brine (up to 71 wt % NaCl eq.) and a vapor. Skarn mineralisation was produced from the brine mixed with meteoric water (215–370°C, up to 23 wt% NaCl eq.). Coeval advanced argillic alteration above the apical part of the granodiorite pluton originated from condensed magmatic vapor (191–367°C, up to 5 wt% NaCl eq.).

Base metal stockwork ore crystallised from fluids showing a positive correlation between salinity (5–0.5 wt.% NaCl eq.) and temperature (330–190 °C), indicative for mixing of magmatic and meteoric fluids, also confirmed by combined O and H isotope data. The absence of boiling due to pressure constraints (granodiorite was still not sufficiently uplifted) could explain the absence of gold in ores.

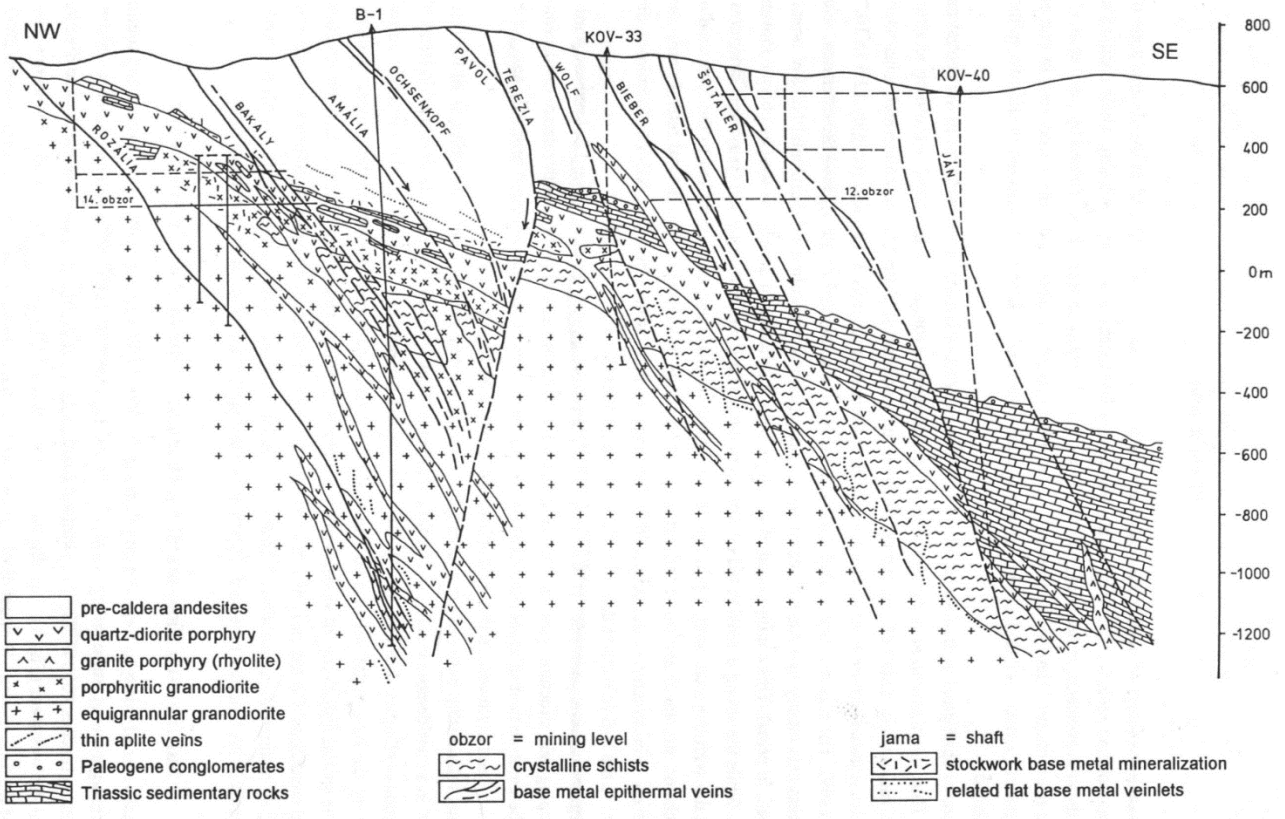


***Figure 12.*** *Transverse sections of the system of sulphide-rich base metal epithermal veins in the Štiavnica ore field SW of Banská Štiavnica (Štohl et al., 1990).*

Fluids associated with the gold-rich, shear-zone hosted veins had salinities (1–4 wt.% NaCl eq.) and temperatures (~250–310 °C) similar to the stockwork. Gold precipitation was mostly induced by boiling of decompressed fluids evolving from suprahydrostatic to hydrostatic conditions at a depth of ~550 m. Boiling in this subhorizontal system of veins was mostly related to opening of dilatational structures that enabled an active suction of fluids and their decompression. The main migration of paleofluids occurred along low-angle normal faults of the shear zone from S–SE to N–NW, as indicated by the geological setting of the quartz-diorite porphyry sills that intruded the shear zone at the end of the hydrothermal activity from S–SE. The main ore mineralisation is associated with areas with densely distributed dilatational structures, where both major boundaries of the shear zone were relatively close together, i.e. where the hanging-wall argillite was relatively close to foot-wall silicite. The strongly argillised upper boundary of the shear zone probably worked as a collector of hydrothermal fluids flowing along the shear zone, as well as a collector of vapour and gases escaping from boiling fluids throughout the entire thickness of the shear zone.

Fluids associated with the base metal horst-related veins have wide ranges of salinities (0.5–11.5 wt.% NaCl eq.) and temperatures (360–110 °C), related to their multistage filling, with evidence for boiling and mixing of fluids.

Magmatic fluids associated with the base metal stockwork and all epithermal mineralisations show increased B, As and Sb contents which indicates that these vapor-affiliated elements were not lost during fluid heterogenisaton on ascent from the magma chamber. Thus, the fluid source was likely supercritical in nature, later contracted to liquid (i.e., they were not lost during fluid heterogenisaton, Fig. 11). Their relatively constant composition indicates a common long-lasting source of fluids exsolved from the magma chamber, also confirmed by stable isotope data. Furthermore, the relatively composition of silicate melt inclusions from corresponding coeval magmatic rocks is in a good agreement with published fluid-melt fractionation factors (Rottier et al., 2019).

### *4.4. Banská Štiavnica – Glanzenberg (medieval excavations)*

This locality represents surficial outcrops of the Au-Ag-Pb-Zn-Cu Špitaler vein, affected by medieval excavations (Fig. 4). It belongs to the system of sulphide rich base metal ± Au veins.

Sulphide rich base metal ± Au veins in surroundings of Banská Štiavnica (“Štiavnica type”) are up to 8 km long, and have a large vertical extent up to 1,000 m (Fig. 12). They dip eastward with the exception of the Terézia vein and some diagonal vein branches dipping westward.

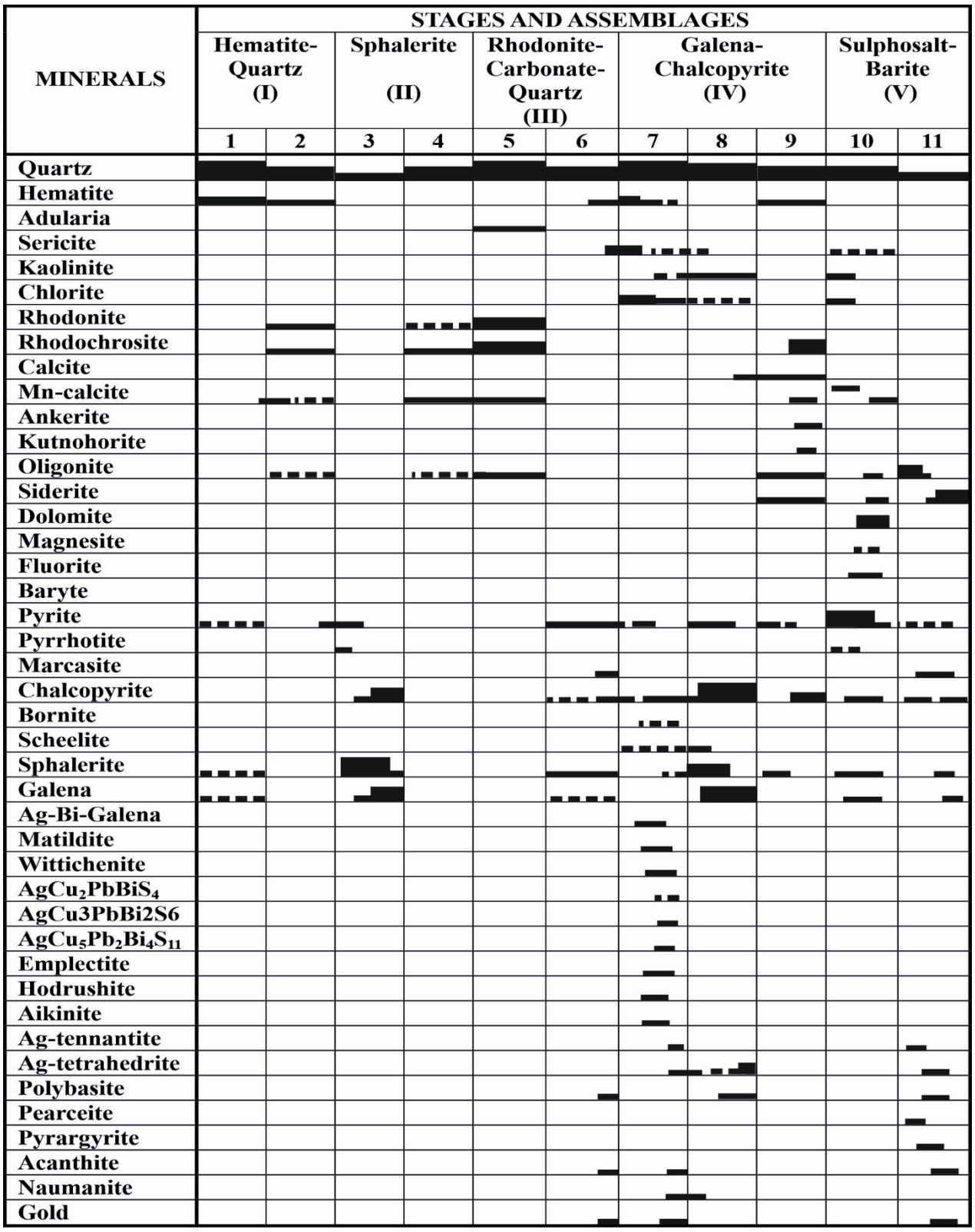


***Figure 13.*** *Paragenetic scheme of the sulphide-rich base metal epithermal veins in the Štiavnica ore field (Kovalenker et al., 1991).*

Vertical displacement on individual veins is in the range of tens to the first hundreds of meter. The veins split often into hanging wall and footwall branches. The maximum thickness of veins in ore shoots may exceed 10 m, exploited were the parts with thickness over 1 m. Veins are represented by mostly cavernous quartz and quartz-carbonate gangue, showing variably breccia, drusy and/or banded crustification textures. Major ore minerals include chalcopyrite, galena, sphalerite, Ag sulphosalts and gold. Vein filling developed during two mineralization cycles including 5 mineralization stages and 11 paragenetic associations on faults with repeated tectonic activation (Fig. 13; Koděra, 1963; Kovalenker et al.,1991). Spatial distribution of the mineralization stages and paragenetic

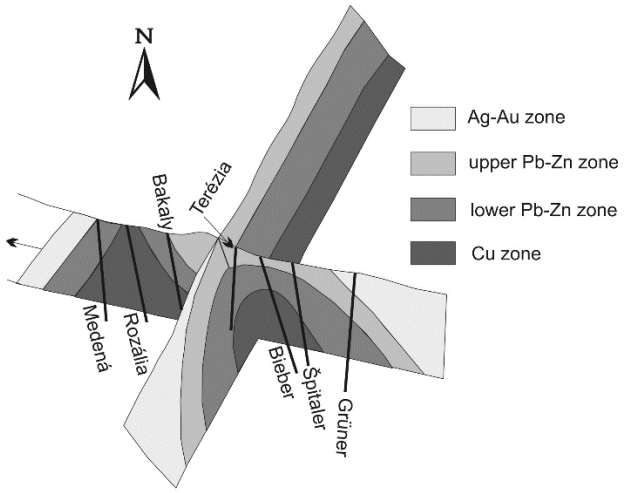


***Figure 14.*** *Vertical zoning of sulphide-rich base metal epithermal veins in the Štiavnica ore field (after Koděra, 1963).*

associations on individual veins has given rise to their general mineral and metallic zoning. Koděra (1963, 1969) distinguished in the vertical sense four zones: upper Au-Ag enriched zone, upper Pb-Zn zone, lower Pb-Zn zone and Cu-zone (Fig. 14). Veins are accompanied by a narrow zone of silicification and adularization, followed by a wider zone of sericitization, passing outward into the zone of propylitization (Onačila et al., 1995).

The Špitaler vein is the longest and the most complex one among the Štiavnica type base metal epithermal veins, exposed here in the upper lead-zinc zone (Lexa, 1999). It is striking NNE-SSW, dipping 60–75° eastward. The vein has numerous hanging wall and footwall branches, forming the vein system up to 50 m wide. Its thickness at the locality is up to 5 m, however, it is split into several closely spaced parallel branches. Thin veinlets follow eventually also the set of antithetic complementary fractures.

Surrounding rocks are propylitized pyroxene andesites of the pre-caldera stage. Close to the vein they are affected by sericitization, adularization and silicification. Zones enriched in pyrite are conspicuous due to hyperfine argillization and bleaching.

Remnants of the quartz-carbonate-sulfide vein filling show variably banded, drusy, cocard or breccia textures. Intermineralization faulting is indicated by crosscutting features and tectonic brecciation. Mineral paragenesis is dominated by base metal sulphides of the 2nd mineralization stage, quartz and carbonates of the 4th mineralization stage and minor silver sulphosalts and electrum of the 5th mineralization stage (Lexa et al., 1997).

## References


Bakos F., Chovan M., Bačo P., Bahna B., Ferenc Š., Hvožďara P., Jeleň S., Kamhalová M., Kaňa R., Knésl J., Krasnec Ľ., Križáni I., Maťo Ľ., Mikuš T., Pauditš P., Sombathy L. & Šály J. (2004): Gold in Slovakia. Slovenský skauting, Bratislava.

Berkh K., Majzlan J., Chovan M., Kozák J. & Bakos F. (2014): Neues Jahrbuch für Mineralogie - Abhandlungen, 191, 237–256.

Chernyshev I.V., Konečný V., Lexa J., Kovalenker V.A., Jeleň S., Lebedev V.A. & Goltsman Y.V. (2013): Geologica Carpathica, 64, 327–351.

Heinrich C.A. (2007): Reviews in Mineralogy and Geochemistry, 65, 363–387.

Kantor J. & Wiegerová V. (1981): Geologica Carpathica, 32, 29–34.

Koděra P., Lexa J., Rankin A.H & Fallick A.E. (2004): Economic Geology, 99, 1745–1770.

Koděra P., Lexa J., Rankin A.H. & Fallick A.E. (2005): Mineralium Deposita, 39, 921–943.

Koděra P., Lexa J., Fallick A.E., Wälle M. & Biroň A. (2014): Geological Society, London, Special Publication 402, 177–206.

Koděra P., Kubač A., Uhlík P., Osacký M., Vojtko R., Chovan M., Lexa J. & Žitňan P. (2017): Proceedings of the 14th Biennial SGA Meeting, vol. 1, 159–162.

Koděra P., Kubač A., Uhlík P., Vojtko R., Chovan M., Lexa J., Milovský R., Laurent O. & Fallick E.A. (2019): Proceedings of the 15th Biennial SGA Meeting, vol. 3, 1042–1045.

Koděra P., Kubač A., Lexa J., Rottier B. & Laurent, O. (2021): Proceedings of the 16th Biennial SGA Meeting, vol. 2, 96.

Koděra P., Lexa J., Chovan M., Vojtko R., Kubač A., Rottier B., Rybárik M. & Prcúch J. (2023): Proceedings 17th Biennial SGA Meeting, 147–150.

Koděra M. (1963): Problems of postmagmatic ore deposition, 1, 184–189.

Koděra, M. (1965): Progress report on the research of mineralogy and geochemistry of the Štiavnica–Hodruša ore district in the year 1964. GÚDŠ Bratislava, 126–128.

Koděra M., Andrusovová–Vlčeková G., Belešová O., Briatková D., Dávidová Š., Fejdiová V., Hurai V., Chovan M., Nelišerová E. & Ženiš P. (1989): Topographic mineralogy of Slovakia, vol. 1. Veda, Bratislava.

Konečný V., Lexa J., Halouzka R., Hók J., Vozár J., Dublan L., Nagy A., Šimon L., Havrila M., Ivanička J., Hojstričová V., Mihaliková A., Vozárová A., Konečný P., Kováčiková M., Filo M., Marcin D., Klukanová A., Liščák P. & Žáková E. (1998a): Explanatory notes to the geological map of Štiavnické and Pohronský Inovec mountain ranges (Štiavnica stratovolcano). D. Štúr Institute of Geology, Bratislava.

Konečný V., Lexa J., Halouzka R., Dublan L., Šimon L., Stolár M., Nagy A., Polák M., Vozár J., Havrila M. & Pristaš J. (1998b): Geological map of the Štiavnické vrchy and Pohronský Inovec Mountains (Štiavnica strato-volcano) 1:50 000. Geological Survey of Slovak Republic, Bratislava.

Konečný V., Lexa J. & Balogh K. (1999): Geolines, 9, 67–75.

Kovalenker V.A., Jeleň S., Levin K.A., Naumov V.B., Prokofjev V.J. & Rusinov V.L. (1991): Geologica Carpathica, 42, 291–302.

Kovalenker V.A., Naumov V.B., Prokofev, V.Y., Jeleň, S. & Haber, M. (2006): Geochemistry International, 44, 118–136.

Kubač A., Chovan M., Koděra P., Kyle J.R., Žitňan P., Lexa J. & Vojtko R. (2018): Mineralogy and Petrology 112, 705–731.

Lexa J. (1999): Society of Economic Geologists, Guidebook Series, 31, 249–258.

Lexa J., Koděra P., Onačila D., Rojkovičová Ľ., Žáková E. & Tréger M. (1997): A complex resource assessment in the Štiavnica stratovolcano central zone. Open file report, D. Štúr Institute of Geology, Bratislava.

Lexa J., Štohl J. & Konečný V. (1999): Mineralium Deposita, 34, 639–665.

Lexa J., Yi K., Broska I., Cieselska Z., Koděra P., Kohút M., Mathur R., Prcúch J., Szczerba M., Uhlík P. & Vojtko, R. (2025): Geologica Carpathica, 76, 1–24.

Majzlan J. (2009): Miner Slovaca, 41, 45–54.

Majzlan J., Berkh K., Koděra P., Števko M., Bakos F. & Milovský R. (2016): Acta Geologica Slovaca, 8, 133–147.

Maťo Ľ., Sasvári T., Bebej J., Kraus I., Schmidt R. & Kalina M. (1996): Mineralia Slovaca, 28, 455–490.

Onačila D., Rojkovičová Ľ., Žáková E., Repčok I., Eliáš K. & Kalinaj M. (1993): Epithermal vein mineralization in the Hodruša ore field. Open file report, D. Štúr Institute of Geology, Bratislava.

Onačila D., Lexa J., Marsina K., Rojkovičová Ľ., Káčer Š., Hojstričová V., Žáková E., Štohl J., Konečný V., Nemčok M., Koděra P., Konečný P., Repčok I., Hurai V., Háber M., Jeleň S., Maťo Ľ., Sasvári T., Schmidt R., Zvara I. & Grant T. (1995): Metalogenetic model and resource assessment of the Štiavnica stratovolcano central zone. Open file report, D. Štúr Institute of Geology, Bratislava.

Rottier B., Audetat A., Koděra P. & Lexa J. (2020): Journal of Volcanology and Geothermal Research, 401, 106967

Šimon L. & Halouzka R. (1996): Geological Magazine, 2, 103–123.

Smolka J. & Lexa J. (2002): Reinterpretation of ore veins within Štiavnica–Hodruša ore district. In: Lexa et al. (eds.): Metalogenetic evaluation of the territory of Slovak Republic. Open file report, D. Štúr Institute of Geology, Bratislava.

Smolka J. et al. (1993): Mineral resource assessment of Slovak Republic – Central Slovakia Volcanic Field. Open file report, D. Štúr Institute of Geology, Bratislava.

Štohl J., Hojstričová V., Lexa J., Rojkovičová Ľ., Žáková E., Gargulák M., Staňa Š., Kantor J. & Ďurkovičová J. (1990): Evaluation of the bore hole B–1 / 2000 m, Horná Roveň. Open file report, D. Štúr Institute of Geology, Bratislava.

Nagybörzsöny
Banská Štiavnica
20 25
15th ASSEMBLY of PETROLOGY
and GEOCHEMISTRY

**We thank our partners for making the conference possible with their financial support!**

Auro-Science Consulting Ltd., Flextra-Lab Ltd., JEOL Europe SAS, Logitech Ltd.,
Stuers GmbH, UNICAM Hungary Ltd., Vacuum Service Ltd.

AURO-SCIENCE CONSULTING

FleXtra LAB

JEOL Solutions for Innovation

LOGITECH Materials Technologists & Engineers

Struers Ensuring Certainty

UNICAM Magyarország Kft.

VACUUM SERVICE KFT.